Doctoral Thesis

博士論文

Control of the rheology and its temperature-sensitivity of wormlike micellar solution of long poly(oxyethylene) chain surfactants

（長鎖ポリ（オキシエチレン）界面活性剤を用いたひも状ミセル溶液

のレオロジー特性およびその温度依存性）

Toufiq Ahmed

トゥフィック　アハメッド

(Student no. 06TB903)

Academic Supervisor:

Assoc. Prof. Dr. Kenji Aramaki

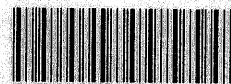*Graduate School of Environment and Information Sciences*

Yokohama National University

横浜国立大学大学院　環境情報学府

September 2009

平成 21 年 9 月

Dedicated to the memory of the late Professor Hironobu Kunieda

Acknowledgement

After thanking the almighty God and then my parents, I wish to express my deep indebtedness to Professor Kenji Aramaki for his constant help and encouragement. I am also grateful the Professors of the Materials Systems Course in the Graduate School of Environment and Information Sciences and my fellow researchers in the laboratory for the kind help they have given me. I also express my sincere thanks to Dr. ANM Hamidul Kabir of the Department of Applied Chemistry and Chemical Technology of the University of Dhaka for his tremendous help he has provided me.

Contents

Chapter 4: Temperature sensitivity of wormlike micelles in poly(oxyethylene) surfactant solution: importance of hydrophilic-group size

Abstract

This thesis details the investigations focused on the rheology and the temperature-sensitivity of the rheology of wormlike micellar solutions formed in aqueous mixtures of long poly(oxyethylene) chain surfactants and hydrophobic cosurfactants. The emphasis is on the variation of the poly(oxyethylene) chain length. The temperature was another important parameter that was varied for the study. Different cosurfactants were used to observe the effect of the change of cosurfactant type on the formation and temperature-dependence of the rheology of wormlike micellar solutions.

Viscoelastic micellar solutions are formed in poly(oxyethylene) cholesteryl ether ($ChEO_m$, m = 15, 30) aqueous solutions upon addition of tri(ethyleneglycol) mono n-dodecyl ether ($C_{12}EO_3$). The steady-shear and dynamic rheological behavior of the systems is characteristic of wormlike micellar solution. In either system, the plateau modulus and relaxation time are found to increase with increasing cosurfactant mixing fractions. The plateau modulus of the $ChEO_{30}-C_{12}EO_3$ system at the maximum viscosity region is found to be higher than that in the $ChEO_{15}-C_{12}EO_3$ system at the maximum viscosity region, whereas for the relaxation time the opposite relation is found. The maximum viscosities obtained in the two systems are of the same order of magnitude. In the $ChEO_{30}-C_{12}EO_3$ system, the maximum viscosity is obtained at a higher cosurfactant mixing fraction than that in the $ChEO_{15}-C_{12}EO_3$ system. It is concluded that decreasing the head-group size of the hydrophilic surfactant favors micellar growth. Monolaurin, another hydrophobic surfactant known to induce growth in some systems, is found to cause phase separation before significant micellar growth occurs in $ChEO_m$ solutions although the effect of head-group size of $ChEO_m$ is found to be similar to the $ChEO_m-C_{12}EO_3$ systems.

Next, we have studied the temperature sensitivity of the rheology of the wormlike micellar solutions formed in poly(oxyethylene) cholesteryl ether ($ChEO_m$, m = 15, 30) upon addition of tri(ethyleneglycol) mono n-dodecyl ether ($C_{12}EO_3$) and monolaurin. We have found that increasing the poly(oxyethylene) chain length of $ChEO_m$ greatly reduces the temperature-sensitivity of the viscosity of the solution. In the viscous region small changes in the cosurfactant composition can subtly change the temperature sensitivity depending on the temperature range and type of cosurfactant. For, $C_{12}EO_3$, which is a poly(oxyethylene) surfactant, the temperature sensitivity is lower at lower temperatures and higher at higher temperatures if the cosurfactant mixing fraction is high and vice versa if the mixing fraction is low. For monolaurin, the temperature sensitivity increases with cosurfactant mixing fraction in the viscous region. In the $ChEO_{30}$-monlaurin system viscous solutions are not formed at any temperature that we studied. We have discussed these results in terms of the reduction of the average curvature of micellar interface with temperature due to dehydration of the poly(oxyethylene) chain and formation of branches in long micelles. We indicate the scientific and technical significance of our findings.

The content of the thesis is based on the following papers:

1. Ahmed, T.; Aramaki, K. "Wormlike micelles in poly(oxyethylene) surfactant solution: Growth control through hydrophilic-group size variation" *J. Colloid Interface Sci.* **2008**, *327*, 180-185 (Chapter 3)

2. Ahmed, T.; Aramaki, K. "Temperature sensitivity of wormlike micelles in poly(oxyethylene) surfactant solution: importance of hydrophilic-group size" *J. Colloid Interface Sci.* **2009**, *336*, 335 - 344 (Chapter 4)

The structure of the thesis is as follows:

Ch. 1: Introduction

⬇

Ch. 2: Experimental

⬇

Ch. 3: Wormlike micelles in poly(oxyethylene) surfactant solution: Growth control through hydrophilic-group size variation.

Ch. 4: Temperature sensitivity of wormlike micelles in poly(oxyethylene) surfactant solution: importance of hydrophilic-group size.

⬇

Ch. 5: Conclusions
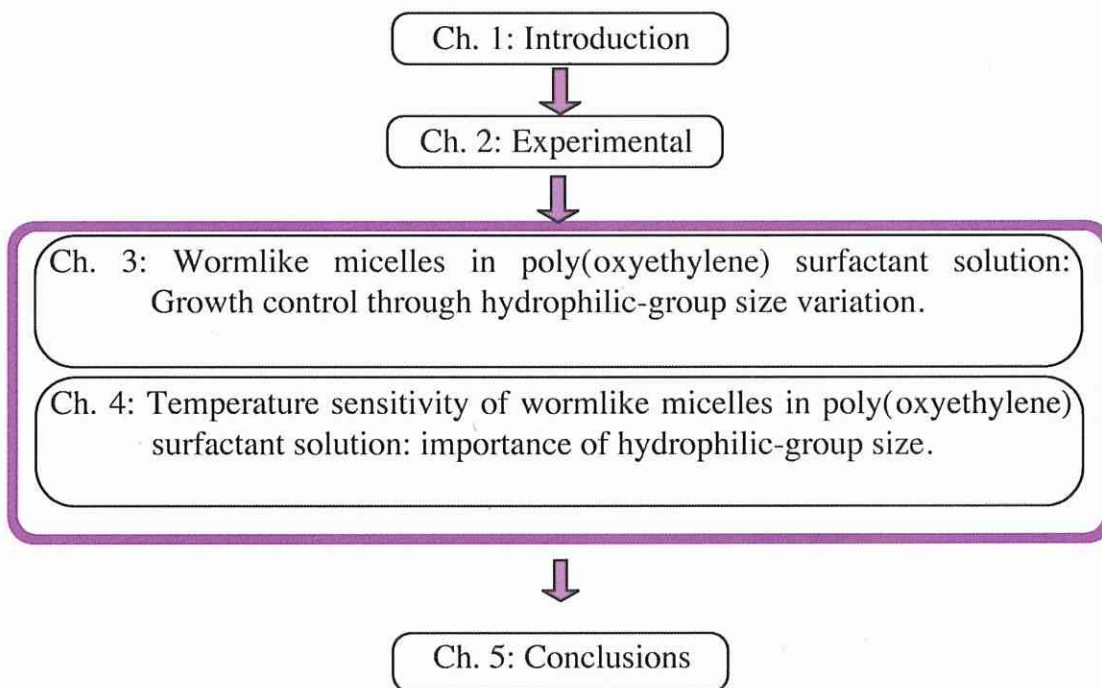
Chapter 1: Introduction

1.1 Amphiphile or Surfactant:

Amphiphiles are molecules having at least one water-soluble (hydrophilic) moiety and one or more water-insoluble (hydrophobic) group. In a homogeneous environment like water, these are in a "frustrated" condition. Therefore, these adsorb spontaneously at the polar-nopolar interface and surfaces, with the hydrophilic groups in contact with the bulk polar phase and the hydrophobic part facing the nonpolar phase. Those amphiphiles that actually do manifest such adsorption behavior are called surface active agents or surfactants.

The hydrophobic part of surfactant usually consists of saturated hydrocarbon chain covalently bonded to hydrophilic moiety. The hydrophilic part of surfactants can vary greatly in chemical structure and compositions. On the basis of the charge of the polar head group surfactants are mainly classified as follows[1,2]:

a) □*Anionics*: these are amphiphilic molecules with an anionic group such as carboxylate, sulfate, phosphate as a polar group coupled with a positive counterion (cation) such as sodium, potassium, ammonium, calcium and protonated alkyl amines. These are the largest group of surfactants.

b) □*Cationics*: these are amphiphiles with cationic group, such as quaternary ammonium as apolar group coupled as a negative counterion (anion) such as halide ion (Cl^-, Br^-). Due to their strong surface activity, they are in surface modification.

c) □*Zwitterionics*: these consist of amphiphile molecules possessing two oppositely charged groups within a single molecule. The cationic group is mostly ammonium ion and the anionic part varies, although carboxylate is the most common.

d) □*Nonionics*: in this class of surfactants the hydrophilic part is a nonionic polar group such as polyether, glycoside or polyhydroxyl. The polyether moiety consists of oxyethylene units, made by polymerization of ethylene oxide (EO). Any material containing an active hydrogen can be ethoxylated, but the most common starting materials are fatty alcohols, alkylphenols, fatty acids and fatty amines. When the number of EO groups is large, the ethoxylation gives a distribution (usually Poisson-type) of EO chain lengths.

Two or more amphiphilic molecules may be connected at the level of head-group or very close to head-group by a spacer group or simply by a covalent bond. These dimeric surfactants, also known as Gemini surfactants, have greater surface activity compared to conventional monomeric surfactants.

The polyether nonionic surfactants, or the POE surfactants, are unique in the sense that their physicochemical properties are very temperature dependent.[1] Contrary to ionic compounds they become less water soluble – more hydrophobic – at higher temperatures. The control of the polymerization of the EO groups that has been achieved allows a systematic variation of the hydrophilic head group size of surfactants, which is very significant for scientific studies.

The field of application of surfactants is one of the widest in modern technology, and involves professionals from diverse areas of science.[1-3] They are used in products as diverse as cosmetics, fertilizers, detergents, paints, dyes, foods, medicines, textiles and play an important role in industrial processes such as mineral and petroleum recovery, pulp and paper production.

1.2 Critical Packing and Geometry of Aggregates

The driving force for the micelle formation in an aqueous system is the hydrophobic interaction between the alkyl chains of the surfactant[4-7] and the interactions that oppose the formation of micelles[8-10] are the electrostatic interaction between the head groups, the steric interaction arising from the packing of head groups at the micelle surface and of alkyl chains in the micelle core, and an interaction associated with residual alkyl chain-water molecules contacts at the micelle surface. The balance between the attractive and repulsive interaction results in the formation of micelles.

From a statistical thermodynamic viewpoint, for a solution of surfactants in aqueous solution with X_N is the mole fraction of surfactant composing aggregates of aggregation number N, $\tilde{\mu}_N^0$ is the standard chemical potential per amphiphile in aggregate of size N, $\tilde{\mu}_N$ is the chemical potential per amphiphile in an N-mer, k_B is the Boltzmann constant, T is the absolute temperature, the following result can be derived:[11]

$$\tilde{\mu}_N = \tilde{\mu}_N^0 + \left(k_B T / N\right)\ln\left(X_N / N\right) = \mu \qquad (1\text{-}1)$$

which takes into account the amphiphilic nature of the surfactants and expresses the important fact that at equilibrium, the chemical potential of all amphiphiles in solution should be independent of their state of aggregation, just as in phase equilibrium. Further, taking into account all association-dissociation processes, e.g., $A_N \rightleftharpoons A_m + A_{N-m}$ etc., the familiar expression of mass-action law of chemical equilibrium can be derived for self-assembling systems:[11]

$$\frac{X_N / N}{X_1^N} = \exp\left[-\frac{N}{k_B T}\left(\tilde{\mu}_1^0 - \tilde{\mu}_N^0\right)\right] \qquad (1\text{-}2)$$

In the limit of very low concentrations, surfactants in solution are monomeric. Above a certain threshold concentration X_c, named the critical micelle concentration (CMC) obtained through the relationship:[11]

$$X_c \approx \exp\left(-\frac{\tilde{\mu}_1^0 - \tilde{\mu}_N^0}{k_B T}\right) \qquad (1\text{-}3)$$

for a minimal aggregation number $\bar{N} \gg 1$, globular micelles composed of 30 – 100 molecules form, while the concentration of monomers remain essentially constant. This minimal aggregation number reflects the cooperative nature of micelle formation. In the case of bilayer forming surfactants, e.g., phopholipids, the number is extremely small and macroscopic aggregates are formed directly.

At a concentration very close to the CMC, the micelles are in general spherical. As the concentration is increased, the micelles may remain spheroidal or grow and become elongated, cylindrical or disk like. The micellar shape is determined by a dimensionless parameter often called "critical packing parameter" (CPP), which is defined as $v/a_s l_c$, where v, l_c are the volume and extended length of a hydrophobic alkyl chain respectively and a_s is the area occupied by a surfactant molecule at the micelle-water interface,[8] a_s is determined by the cross-sectional area of the surfactant head group and by the various interactions that play in the micelle formation.[8] On the other hand, the extended length of the alkyl chains for a saturated hydrocarbon with n carbon atoms, l_{max}, and volume v can be estimated by Tanford's equation.[5]

$l_c \leq l_{max} \approx 0.154 + 0.1265n$ nm $\qquad (1\text{-}4)$

$v \approx (27.4 + 26.9n) \times 10^{-3}$ nm^3 $\qquad (1\text{-}5)$

The extended length l_c is approximately 80% of the l_{max} value. Once the cpp of a surfactant molecule is roughly estimated from the molecular dimensions, it gives a

4

rough idea about the shape of the aggregates into which it is packed as shown in Figure 1.1.
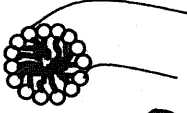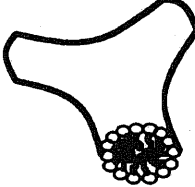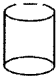
Micellar geometries	Packing parmeter	Surfactant shape	Micellar shape
Globular End-cap	$P < 1/3$		
Cylindrical section	$1/3 < P < 1/2$		
Threefold junction	$1/2 < P < 1$		
Lamellar sheet	$P = 1$		

Figure 1.1: Schematic representation of the shape of the surfactant and self-assembled structures depending on the critical packing parameter

The hydrophilic head group on the side of water interface and hydrophobic tail on the other side of the interface determines an optimal curvature, also, known as spontaneous curvature, which in turn determines geometry of the aggregates. The principle curvatures, c_1 and c_2, define the mean ($H = (c_1 + c_2)/2$) and the Gaussian ($K = c_1 c_2$) curvatures. Aggregates enclosing polar head groups and water (reverse micelles) are regarded to have negative curvatures; on the other hand, the aggregates with interior filled with lipophilic chains (normal micelles) have positive curvatures. By convention, normal micellar aggregates with $cpp < 1$, have a normal or positive curvature, whereas the reverse aggregates with $cpp > 1$, are considered to have reversed or negative curvatures. An interesting case is $1/2 < cpp < 1$, which allows the

possibility of branched cylindrical micelle formation. A simple general expression relates the dimensionless packing parameter to the curvature of the interface:

$$CPP = \frac{v}{a_s l_c} = 1 - H l_c + \frac{K l_c^2}{3} \qquad (1\text{-}4)$$

Alternately,

$$CPP = \frac{v}{a_s l_c} = 1 - \frac{1}{2}\left(\frac{1}{R_1} + \frac{1}{R_2}\right) l_c + \frac{l_c^2}{3 R_1 R_2} \qquad (1\text{-}5)$$

where R_1 (=$1/c_1$) and R_2 (= $1/c_2$) are the radii of local curvatures.

The micellar growth with surfactant concentration has been explained by different models, which all assume that the free energy of a surfactant is higher in spherical micelles than in rodlike or disk like micelles.[8-10] The larger the magnitude of the free energy difference, the steeper is the increase of the micellar size with increasing surfactant concentration. The surfactants with $CPP > 1/3$ shows micellar growth with the surfactant concentration. Besides, ionic surfactants with a value of CPP slightly below $1/3$ may show micellar growth. It is noteworthy to point out that the polydispersity in the size of the micelles largely depends on the shape of the aggregate structure. As generally accepted, the polydispersity of the spherical micelles is smaller compared to the elongated, cylindrical or lamellar micelles.

1.3 One-dimensional micellar growth

The concept of elongated, or rodlike, micelles was introduced as early as 1951 by the great Peter Debye.[12] They concluded, based on light scattering studies, that cetyltrimethylammonium bromide in aqueous potassium bromide form micelles that are rodlike in shape, rather than being spherical or disk-shaped.That elongated micelles may form entangled network structure with high solution viscosity was

suggested quite early by N. Pilpel in 1956.[13] Thus, the concept of elongated micelles

is not new. However, the theoretical and experimental achievements of recent years

have made the study of these systems quite fascinating.

The thermodynamic incentive for micellar growth is the different packing

energies in the cylindrical part and the curved end-regions. The energy required for

breaking a linear micelle into two shorter micelles is denoted 2δ. Performing a free

energy calculation with due consideration to the end-energy, the weight average

micellar size, defined by, $\langle N \rangle = \int_0^\infty X(N) N \, dN \,/\, \int_0^\infty X(N) \, dN$ is found to be:[11]

$$\langle N \rangle = 2 e^{\delta / k_B T} \sqrt{X} = 2N^* \qquad (1\text{-}6)$$

where N^* is the most probable aggregation number. Alternatively, using mean-field

theory it can be found for the free energy density F:[14]

$$\beta F = \sum_N c(N) \left[\ln c(N) + \beta E \right] + F_0(\phi) \qquad (1\text{-}7)$$

where $c(N)$ is the number density of aggregates of N monomers and $E = 2\delta$, ϕ is the

total volume fraction, $\beta = 1/k_B T$. Minimizing the above equation at fixed ϕ gives

$$c(N) \propto \exp\left[-N / \overline{N} \right]; \quad \overline{N} \simeq \phi^{1/2} \exp\left[\beta E / 2 \right] \qquad (1\text{-}8)$$

where $\overline{N}$ is the number average aggregation number. For branched micelles with z-

fold branches the result is modified as:[15]

$$\beta F = \sum_N c(N) \left[\ln c(N) + \beta E z^{-1} \right] + 2 \left(z^{-1} - 1 \right) C \ln(2C) + F_0(\phi) \qquad (1\text{-}9)$$

Thus the main ingredient for micellar growth is the increase in the end-cap

energy.[8, 11] This can be achieved by several different methods. The most studied

involves ionic surfactants in the presence of salts of both binding (e.g. sodium

salicylate) and non-binding type.[16-25] The mechanism involved in this formation is the

screening of the electrostatic repulsions between the charged head-groups, leading to

an increase in the end-cap energy. Consequently, the average micellar length increases dramatically. Wormlike micelles can also form in mixtures of a surfactant with another small molecules called hydrotropes. Incorporation of co-surfactant with a small head-group in the palisade layer of micellar aggregates of ionic surfactants reduces the effective area per molecule a_s, which results in an increase of *CPP*, thus leading to micellar growth.[26-31] Nonionic surfactants can also form wormlike micelles, usually in the presence of co-surfactants.[32-44] Mixtures of oppositely charged surfactants often exhibit synergistic enhancement of the rheological properties. The micellar growth can occur by decrease in the micellar surface potential via charge neutralization and increase in ionic strength by the release of counterions.[45-47] Mixtures of ionic and non-ionic surfactants can also display synergistic effects and have been studied extensively.[48-51] Zwitterionic surfactants that contain both positive and negative charges can also form wormlike micelles.[52, 53] Gemini or dimeric surfactants have been found to form wormlike micelles.[54, 55] The result of these extensive studies is that the counterion with strong binding capability is more suitable for micellar growth in ionic system and the co-surfactant with the smaller head-group or longer hydrophobic tail (within a small range of variation) gives better growth. The case of the cationic/anionic mixture can be considered to be an extreme case of ionic surfactant with binding salts.[56, 57]

The effect of temperature on the micellar growth can be understood from the relationships given in equations (1-7) to (1-9). For most common surfactants, the end-cap energy is not affected by the temperature and therefore the micellar contour length decreases exponentially with temperature rise.[22, 58, 59] A notable exception is poly(oxyethylene) surfactants, whose head-groups become effectively smaller with rise in temperature due to dehydration of the oxyethylene units. This means a

reduction of the micellar interfacial curvature, and so temperature-induced growth is to be expected. This is indeed observed in several systems.[60-62] However, very highly viscous wormlike micellar solution is rare in poly(oxyethylene) surfactants and therefore there is room for research in this field.

The scattering of X-ray, light and neutrons by matter due to static or dynamic heterogeneities in material is a very useful method for understanding the microscopic structure and dynamics. Briefly, an incident beam of radiation is scattered by the material with different intensities at different angles. The variation of the intensity with angle provides information on the microstructure responsible for scattering. Increasingly smaller length-scales are probed at larger scattering angle. Usually, scattering data, presented as a function of the scattering vector given by $q = 4\pi\sin\theta/\lambda$ (θ = scattering angle, λ = wavelength of radiation), display variation over many order of magnitude of q. Since light and neutron have different wavelengths, the two can be complementary for investigating different length-scales, as can be understood from the definition of q.[63] For low surfactant concentration, the micelles are free from significant interactions, and the interpretation of the data is quite easy and reliable.[63,64] The micellar contour length, persistence length and cylinder cross-section diameter has been extracted from the scattering data of dilute solutions.[65] For concentrated solutions, the successful application of Renormalization-group theory for flexible polymers by Schurtenberger and co-workers to the SANS, SLS and DLS data of wormlike micelles gives one of the strongest support of the formation of polymer-like micelles as well as providing a non-invasive method of characterizing such systems.[66,67] The exponent ½ in equation 1-8, derived from mean-field theory, has been demonstrated by scattering experiments to be invalid when interaction among

9

micelles is strong.[17, 32, 63, 66] Modern simulation methods have been utilized to analyze and model the data. Thus, indeed the study of wormlike micelles can provide important model systems for testing modern molecular theories.

We would like to point out the existence of another group of materials having similarity in structure and dynamics with those of solutions of long micelles. Several examples of hydrogen-bonded supra-molecular polymers are known: benzene-tricarboxamide or cycloheaxane-tricaboxamide in n-alkanes, cyclohexane or toluene; bis-ureas in toluene.[68-71] Whereas the self-assembly of wormlike micelles is controlled by a delicate balance of the various geometric aspects of the head-group and the tail, the structure of the monomer of supra-molecular polymer can be considered to be composed of two almost non-interacting components – the associating groups responsible for the self-assembly process, and the rest of the molecule, free to be altered at will without compromising the self-assembly process. Therefore, the formation of wormlike micelles is more difficult than the development of supra-molecular polymer solutions.

1.4 Rheological behavior of micellar solutions

Surfactant molecules self-assemble into aggregates of different microstructures depending on the composition, temperature, and other outer conditions. At a surfactant concentration just above critical micelle concentration (CMC), micelles are usually in spherical shape. The micellar solutions with globular aggregates always have a low viscosity, often comparable to the viscosity of the solvent (η_s). The viscosity (η) varies linearly with the volume fraction of the globular particles, ϕ, according to the Einstein's equation:

$$\eta = \eta_s (1+2.5\phi) \hspace{3cm} (1\text{-}10)$$

The rodlike aggregates increase the viscosity slightly as long as they do not overlap. The sphere-rod transition in the micellar shape can be induced by different ways such as increasing surfactant concentrations, salinity or temperature, depending on the type of the surfactant. At certain conditions, these micelles can undergo elongation to form long and flexible aggregates called as 'threadlike' or 'wormlike' micelles.

Figure 1.2: Schematic diagram of non-entangled (concentration $< c^*$), and entangled (concentration $> c^*$) wormlike micelles.

Above a certain surfactant concentration, called overlap concentration (c^*), the wormlike micelles begin to overlap with each other and viscosity becomes much higher than that predicted by the Einstein's equation. In some surfactant solutions, the viscosity may be very high even at low concentrations (about 1 wt%) suggesting a supramolecular three-dimensional network structure. Formation of such a structure is attributed to the tendency of the micellar aggregates to arrange them into long threadlike or wormlike aggregates, which are connected and interwoven or entangled to form a transient network (Figure 1.2). The entanglement of the flexible aggregates to form a transient network analogous to the polymer network imparts a viscoelastic behavior to the solution, that is, simultaneous coexistence of viscous and elastic properties. The presence of the viscoelasticity manifests in phenomenon such as rod climbing and elastic recoil, as well as the presence of entrapped bubbles in the sample. The presence of long chain is a necessary but not a sufficient condition for

viscoelasticity. The structure must also possess a certain internal mobility to relax the stress imposed on the system and a permanence of the structure is also necessary to maintain elastic properties.

The wormlike micelles have an equilibrium conformation in the networks. The micelles constantly undergo translational diffusion process, and they also break and recombine. If the network is deformed or equilibrium conditions are suddenly changed, the relaxation occurs within a definite time and the equilibrium condition is restored again. If the network is deformed by a small perturbative shear stress σ in a shorter time than it can reach equilibrium, the system exhibit elastic property characteristics of a solid material with a Hookean constant G_0, which is called the shear modulus, and we obtain a simple relation between stress (σ) and strain (γ):

$$\sigma = G_0 \, \gamma \qquad\qquad (1\text{-}11a)$$

If, on the other hand, the network is deformed slowly, it behaves like a viscous fluid with a zero-shear viscosity η_0 and the shear stress is given by

$$\sigma = \eta_o \frac{d\gamma}{dt} \qquad\qquad (1\text{-}11b)$$

where $(d\gamma/dt)$ is the shear rate.

The dynamic rheological behavior of viscoelastic micellar solution is described by the mechanical model, called the Maxwell model, consisting of an elastic component (spring) with the Hookean constant G_0 and a viscous component (dashpot) with the viscosity η_0 [Figure]. When a sudden strain is applied to the system for a short time, the stress relaxes exponentially with a time constant τ_R

$$\sigma = \sigma_o \exp(-t/\tau_R) \qquad\qquad (1\text{-}12)$$

$$\tau_R = \eta_0 / G_0 \qquad\qquad (1\text{-}13)$$

It is possible to obtain different rheological parameters by following the stress decay as a function of time. Alternatively, the rheological properties of a viscoelastic material can be investigated by applying a sinusoidal deformation of angular frequency ω. From the phase angle between sinusoidally varying stress and strain signals, the elasticity (storage) modulus G', the viscous (loss) modulus G'', and the magnitude of complex viscosity $|\eta^*|$ can be calculated. For a Maxwell fluid, following relations are obtained:[72]

$$G'(\omega) = \frac{\omega^2 \tau_R^2}{1 + \omega^2 \tau_R^2} G_0 \qquad \text{(1-14)}$$

$$G''(\omega) = \frac{\omega \tau_R}{1 + \omega^2 \tau_R^2} G_0 \qquad \text{(1-15)}$$

$$|\eta^*| = \frac{(G'^2 + G''^2)^{1/2}}{\omega} = \frac{\eta_o}{\sqrt{1 + \omega^2 \tau_R^2}} \qquad \text{(1-16)}$$

where ω is the frequency of oscillatory-shear. G_0 is called shear (plateau) modulus. At low ω, and $\omega\tau_R \ll 1$, G' becomes proportional to ω^2 whereas G'' is proportional to ω, with $G'' > G'$. This region is called a terminal zone, and the system behaves as a simple liquid (Figure 1.3(a)). It can be seen that for $\omega\tau_R \gg 1$, G' approaches a constant limiting plateau value equal to shear modulus (G_0), with $G' > G''$ and the system behaves as an elastic material. The G_0 is a material property and is related to the number density of entanglement (v) at a temperature T, according to the following relation:

$$G_0 = v\,kT \qquad \text{(1-17)}$$

where k is the Boltzmann constant.

The relaxation time, τ_R, is given by the inverse of the ω (expressed in rad.s^{-1}) corresponding to G'-G'' cross-over in a G', G''-ω plot. In addition to equation (1-13),

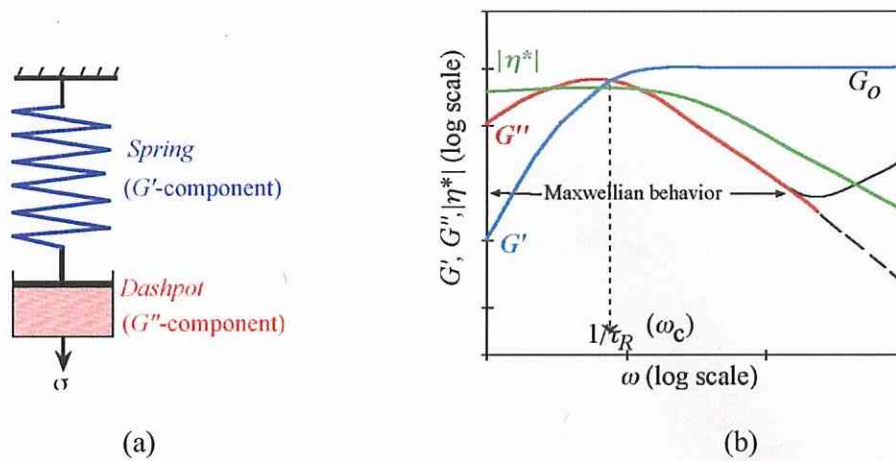(a)   (b)

Figure 1.3: (a) Mechanical model for a viscoelastic behavior described by the Maxwell equations. (b) The rheological behavior shown by a typical wormlike micellar solution. At low oscillatory-shear frequency the system shows the Maxwellian behavior. However, at high frequency deviation from the Maxwellian behavior is observed.

equation (1-16) allows one to estimate η_o from the oscillatory-shear measurement by extrapolating $|\eta^*|$ to the zero oscillatory frequency.

Although the Maxwell equations predict a monotonous decrease of G'' at a high frequency region [shown by a broken line in Figure 1.3(b)], the wormlike micelles deviate from this behavior, showing an upturn of G'' in high-frequency region [shown by solid line in Figure 1.3(b)]. This deviation is often associated with the transition of relaxation mode from 'slower' reptation to other 'faster' processes such as Rouse modes of cylindrical micelles, analogous to a polymer chain. The minimum value of G'' at high-frequency region is related to the micellar contour length according to the following relation:[14]

$$\frac{G''_{min}}{G_o} \approx \frac{l_e}{L} \tag{1-14}$$

14

where l_e is the entanglement length, i.e., the contour length of the section of wormlike micelles between two entanglements, and $\overline{L}$ is the contour length of the wormlike micelle. For flexible micelles, the correlation length, ξ which gives the mesh size of the micellar network, is related to l_e and G_0 according to the relations [14, 73]

$$l_e \approx \frac{\xi^{\frac{5}{3}}}{l_p^{\frac{2}{3}}}$$

(1-18)

$$\xi \approx \left(\frac{kT}{G}\right)^{\frac{1}{3}}$$

(1-19)

Combining Eqs. (1-18) and (1-19) yields a relation which relates G_0 to l_e

$$G_0 \approx \left(\frac{kT}{l_e^{\frac{9}{5}}}\right)$$

(1-20)

The living polymer model proposed by Cates et $al^{[14,\ 73]}$ describes the viscoelastic behavior of entangled wormlike micelles by considering two processes of stress relaxation – reptation or reptile-like motion of the micelle along its own contour, and reversible scission of micelles – taking place at two time scales, namely, reptation time τ_{rep} and breaking time τ_b. When the time scale of breaking and recombination of micelles occurs in a very short time scale in comparison to the slow reptation process, that is, $\tau_{rep} >> \tau_b$, the viscoelastic behavior of such a system at low shear frequency follows the Maxwell model with single relaxation time τ_R given by $(\tau_b.\ \tau_{rep})^{1/2}$. In the limit $\tau_b >> \tau_{rep}$, the theoretical model predicts the following scaling laws for the viscoelastic parameters as a function of the fraction of surfactant (ϕ).

1.5 Significance of the present work

Due to the functionality, surfactants have become indispensable in all aspects of modern technology and society. Therefore, the risk of exposure to such substances for the environment and human health should be given good considerations. Also, the environmental impact of the manufacture of surfactants should be thought about. A general guideline is to choose materials that are biodegradable and can be produced from renewable resources. In this respect, the poly(oxyethylene) cholesteryl ether surfactants are very attractive because the cholesteryl group is derived from plant materials. Also, both the hydrophobic and the hydrophilic groups are rather harmless to the environment. Therefore, their application and study should be welcome. Viscoelastic wormlike micellar solutions, in particular, now find application in foods, cosmetics, pharmaceuticals, oil-fields etc. So, the potential for highly viscous solutions of poly(oxyethylene) cholesteryl ethers should be given much attention.

More important from the scientific standpoint is that the scattering studies of wormlike micelles of ionic surfactants, as well as the computer simulation and interpretation of rheological data of charged amphiphile solutions are complicated due to electrostatic interactions. Cates' model applies properly to nonionic wormlike micelles. Therefore, development of wormlike micellar systems based on nonionic surfactants is very important in order to understand the structure and dynamics of this important class of material. Among nonionics, the poly(oxyethylene) type form the largest class. But only poly(oxyethylene) cholesteryl ether surfactants are known to form very highly viscous ($\sim 10^3$ Pa·s) wormlike micellar solution upon addition of proper co-surfactants. As mentioned previously, the poly(oxyethylene) group manifests interesting temperature induced change in effective size. This in turn, affects the curvature of the micellar interface and the temperature effect on the

rheology of wormlike micellar solution of this surfactant is different from other surfactant groups.

In order to utilize the uniqueness of poly(oxyethylene) cholesteryl ether surfactants in the study of micellar growth and temperature sensitivity, it is important to be able to form highly viscous solutions from very long POE chain surfactants using nonionic co-surfactants. This can provide the opportunity to tune the structural parameters such as contour length, persistence length, cross-sectional diameter of wormlike micelles over a wide range by varying the POE chain length. Also, since it is known that the effect of temperature on the micellar growth in poly(oxyethylene) alkyl ether depends on the POE chain length, the temperature effect on the rheology of wormlike micelles of very long POE chain cholesteryl ether should be compared with that of shorter chain homologues.

Appendix: Viscoelasticity of living polymer

In the theory of entangled polymer solutions a basic quantity is the stress-relaxation function $\mu(t)$, which is the fraction of imposed stress remaining at time t after an infinitesimal stress is imposed at time 0. The $\mu(t)$ is basically the average fraction of tube existing at time 0 that has not been lost by disengagement by time t. The portions of the original tube persisting at time t are those through which neither end of the chain has passed. The problem is equivalent to a one-dimensional stochastic problem if we imagine the chain to be at rest in a moving tube, to convert $\mu(t)$ to be the survival probability of a particle with diffusion constant equal to the curvillinear diffusion constant D_c of the chain, launched at $t = 0$ with uniform probability on the line segment [0, L] with boundaries that absorb the particle. For Worm-like micelles, Cates extended this idea by allowing the absorbing boundaries to undergo jump transitions with probabilities given by the rate constants of bond-exchange processes. Even without solving the resulting equations some important conclusions can be reached. For $\tau_b <<$

τ_{rep} the $\mu(t)$ is the probability that an arbitrary tube segment, present at $t = 0$, survives to time t without a chain end passing through it. However, the tube segments need only to wait for a break to occur close enough to it, so that the new chain end can pass through the given tube segment before disappearing again. The distance l an end can move by reptation during its lifetime τ_b obeys $D_c(L)l^2 \approx \tau_b$ and so $(l/L)^2 \approx \tau_b/\tau_{rep}(L)$ due to ordinary reptation theory. The waiting time τ for a new end to appear within l is $\tau_b L/l$. This gives, for a characteristic stress relaxation time $\tau_b \approx (\tau_b \tau_{rep})^{1/2}$.

References

1.☐ Holmberg, K.; Jönsson, B.; Kronberg, B.; Lindman, B. *Surfactants and Polymers in Aqueous Solution*, John Wiley & Sons. New York, **1998**.

2.☐ Rosen M. *Surfactants and Interfacial Phenomena*, John Wiley, New York, 2nd edition **1989**.

3.☐ Evans, D. F.; Wennerstrom, H. *The Colloidal Domain: Where Physics, Chemistry and Biology Meet*, VCH Publishers: New York, 1994

4.☐ Hartley, G.S. Aqueous Solutions of Paraffinic-Chain Salts. *A Study of Micelle Formation*, Herman, Paris, **1936**.

5.☐ Tanford, C. *The Hydrophobic Effect*, John Wiley and Sons, New York, **1980**.

6.☐ Chandler, D. *Nature* **2002**, *417*, 491.

7.☐ Chandler, D. *Nature* **2005**, *437*, 640.

8.☐ Israelachvili, J.; Mitchell, D.J.; Ninham, B.W. *J. Chem. Soc., Faraday Trans.* **1976**, *72*, 2978.

9.☐ Nagarajan, R.; Ruckenstein, E. *Langmuir* **1991**, *7*, 2934.

10.☐Shiloah, A.; Blankschtein, D. *Langmuir* **1998**, *14*, 7166.

11.☐May, S.; Ben-Shaul, A., in *Giant Micelles Properties and Applications*; Zana, R.; Kaler, E. W., Eds.; CRC Press: **2007**; Chapter 2.

12.☐Debye, P., Anacker, E. W., *J. Phys. Colloid Chem.* **1951**, *55*, 644

13.☐Pilpel, N. *J. Phys. Chem.* **1956**, *60*, 779

14. Cates, M.E.; Candau, S.J. *J. Phys. Condens Matter* **1992**, *2*, 6869.

15. Drye, T. J.; Cates, M.E., *J. Chem. Phys.* **1992**, *96*, 1367.

16. Arleth, L.; Bergstrom, M.; Pedersen, J.S. *Langmuir* **2002**, *18*, 5343.

17. Magid, L.; Li, J.Z.; Butler, P.D. *Langmuir* **2000**, *16*,10028.

18. Berlepsh, H. Von; Dautzenberg, H.; Rother, G.; Jäger, J. *Langmuir* **1996**, *12*, 3613.

19. Candau, S.J.; Hirsch, E.; Zana, R.; Adam, M. *J. Colloid Interface Sci.* **1988**, *122*, 30.

20. Quirion, F.; Magid, L.J. *J. Phys. Chem.* **1986**, *90*, 5435.

21. Mu, J.-H.; Li, G.-Z.; Jia, X.-L.; Wang, H.-X.; Zhang, G.-Y. *J. Phys. Chem. B* **2002**, *106*, 11685.

22. Raghavan, S.R.; Kaler, E.W. *Langmuir* **2001**, *17*, 300.

23. Croce, V.; Cosgrove, T.; Maitland, G.; Hughes, T.; Karlsson, G. *Langmuir* **2003**, *19*, 8536.

24. Siriwatwechakul, W.; Lafleur,T.; Prudhhomme, R.K.; Sullivan, P. *Langmuir* **2004**, *20*, 8970.

25. Schubert, B.A.; Wagner, N.J.; Kaler, E.W.; Raghavan, S.R. *Langmuir* **2004**, *20*, 3564.

26. Porte, G.; Gomati, R.; Haitamy, O.El.; Appell J.; Marignan, J. *J. Phys. Chem.* **1986**, *90*, 5746.

27. Douliez, J.P.; Navailles, L.; Nallet, F. *Langmuir* **2006**, *22*, 622.

28. Thiele, T.; Berret, J.-F.; Muller, S.; Schmidt, C. *J. Rheol.* **2001**,*45*, 29.

29. Singh, M.; Ford, C.; Agarwal, V.; Fritz, G.; Bose, A.; John, V.T.; McPherson, G.L. *Langmuir* **2004**, *20*, 9931.

30. Couillet, I.; Hughes, T.; Maitland, G.; Candau, F.; Candau, S.J. *Langmuir* **2004**, *20*, 9541.

31. Miyake, M.; Einaga, Y. *J. Phys. Chem. B* **2007**, *111*, 535.

32. Stradner, A.; Glatter, O.; Schurtenberger, P. *Langmuir* **2000**, *16*, 5354.

33. Acharya, D.P.; Sharma, S.C.; Rodriguez-Abreu C.; Aramaki, K. *J. Phys. Chem. B* **2006**, *41*, 20224.

34. Sato, T.; Acharya, D.P.; Kaneko, M.; Aramaki, K.; Singh,Y.; Ishitobi, M.; Kunieda, H. *J. Dispersion Sci. Technol.* **2006**, *27*,611.

35. Kunieda, H.; Umizu, G.; Aramaki, K. *J. Phys. B* **2000**, *104*, 2005.

36. Kunieda, H.; Horii, M.; Koyama, M.; Sakamoto, K. *J. Colloid Interface Sci.* **2001**, *236*, 78.

37. Rodriguez-Abreu, C.; Aramaki, K.; Tanaka, Y. López-Quintela, M.A. Ishitobi, M.; Kunieda, H. *J. Colloid Interface Sci.* **2005**, *291*, 560.

38. Maestro, A.; Acharya, D.P.; Furukawa, H.; Gutierrez, J.M.; López-Quintela, M.A.; Ishitobi, M.; Kunieda, H. *J. Phys.Chem. B* **2004**, *108*, 14009.

39. Kunieda, H.; Rodriguez, C.; Tanaka, Y.; Kabir, Md.H.; Ishitobi, M. *Colloids Surf. B* **2004**, *38*, 127.

40. Acharya, D.P.; Kunieda, H. *J. Phys. Chem. B* **2003**, *107*,10168.

41. Moitzi, C.; Freiberger, N.; Glatter, O. *J. Phys. Chem. B*, **2005**,*109*, 16161.

42. Acharya, D.P.; Hossain, Md.K.; Feng, J.; Sakai T.; Kunieda, H. *Phys. Chem. Chem. Phys.* **2004**, *6*, 1627.

43. Naito, N.; Acharya, D.P.; Tanimura J.; Kunieda, H. *J. Oleo Sci.* **2004**, *53*, 599.

44. Naito, N.; Acharya, D.P.; Tanimura J.; Kunieda, H. *J. Oleo Sci.* **2005**, *54*, 7.

45. Bergstrom M.; Pedersen, J.S. *Langmuir* **1999**, *15*, 2250.

46. Koehler, R.D.; Raghavan, S.R.; Kaler, E.W. *J. Phys. Chem.B* **2000**, *104*, 11035.

47. Raghavan, S.R.; Fritz G.; Kaler, E.W. *Langmuir* **2002**, *18*, 3797.

48. Acharya, D.P.; Sato, T.; Kaneko, M.; Singh Y.; Kunieda, H. *J. Phys. Chem. B* **2006**, *110*, 754.

49. Engelskirchen, S.; Acharya, D.P.; Garcia-Roman, M.; Kunieda, H. *Colloids Surf. A* **2006**, *279*, 113.

50. Acharya, D.P.; Hattori, K.; Sakai, T.; Kunieda, H. *Langmuir* **2003**, *19*, 9173.

51. Rodriguez, C.; Acharya, D.P.; Hattori, K.; Sakai, T.; Kunieda, H. *Langmuir* **2003**, *19*, 8692.

52. Hoffmann, H.; Rauschera, A.; Gradzielski, M.; Schulz, S.F. *Langmuir* **1992**, *8*, 2140.

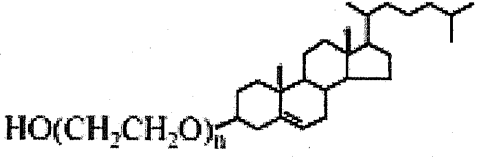53. Fischer, P.; Rehage, H.; Gruning, B. *J. Phys. Chem. B* **2002**, *106*, 11041.

54. Oda, R.; Huc, I.; Homo, J.C.; Heinrich, B.; Schmutz, M.; Candau, S. *Langmuir* **1999**, *15*, 2384.

55. Acharya, D.P.; Kunieda, H.; Shiba, Y.; Aratani, K. *J. Phys.Chem. B* **2004**, *108*, 1790.

56. Kaler, E. W.; Herrington, K. L.; Murthy, A. K.; Zasadzinski, J. A. N. *J. Phys.Chem.* **1992**, *96*, 6698.

57. Schubert, B. A.; Kaler, E, W.; Wagner, N.J. *Langmuir* **2003**, *19*, 4079.

58. Kern, F.; Zana, R.; Candau, S. J. *Langmuir* **1991**, *7*, 1344.

59. Kern, F.; Lequeux, F.; Zana, R.; Candau, S. J. *Langmuir* **1994**, *10*, 1714.

60. Sato, T.; Hossain, Md.K.; Acharya, D.P.; Glatter, O.; Chiba, A.; Kunieda, H. *J. Phys. Chem. B* **2004**, *108*, 12927.

61. D. P. Acharya , D. Varade , K. Aramaki , *J. Colloid and Interface Science* **2007**, *315*, 330

62. Varade, D.; K. Ushiyama, L. K. Shrestha, K. Aramaki, *J. Colloid Interface Sci.* **2007** *312*, 489.

63. Jerke, G.,; Pedersen, J. S.; Egelhaf, S. U.; Schurtenberger, P. *Phys. Rev. E* **1997**, *56*, 5772.

64. Berlepsh, H. Von; Mittelbach, R.; Hoinkis, E.; Schnablegger, H. *Langmuir* **1997**, *13*, 6032.

65. Chen, W.R.; Butler, P.D.; Magid, L.; *Langmuir* **2006**, *22*,6539.

66. Schurtenberger, P.; Cavaco, C. J. *J. Phys. II (France)* **1993**, *3*, 1279.

67. Schurtenberger, P.; Cavaco, C. J. *J. Phys. II (France)* **1994**, *4*, 305.

68. Shikata, T.; Ogata, D.; Hanabusa, K. *J. Phys. Chem. B* **2004**, *108*, 508.

69. Hanabusa, K.; Kawakami, A.; Kimura, M.; Shirai, H. *Chem. Lett.* **1997**, 191.

70. Ducouret, G.; Chassenieux, C.; Martins, S.; Lequeux, F. ;Bouteiller, L. *J. Colloid Interface Sci.* **2007**, *310*, 624.

71. Gucht, v. d. J.; Besseling, N. A. M.; Knoben, W.; Bouteiller, L.; Cohen S. M. A. *Phys. Rev. E* **2003**, *67*, 051106.

72. Larson, R.G. *The Structure and Rheology of Complex Fluids*, Oxford University Press, New York, **1999**.

73. Granek, R.; Cates, M. E. *J. Chem. Phys.* **1992**, *96*, 4758.

Chapter 2: Experimental

2.1 Materials

◆ <u>Surfactants used in the present study are given in the following table.</u>

Table 2-1: List of amphiphiles used in the studies included in this thesis.

Amphiphiles	Formula	Abbreviation
Poly(oxyethylene) cholesteryl ether	$HO(CH_2CH_2O)_n$	$ChEO_n$ n = 15, 30
Monolaurin (Glycerol α-monolaurate)	$C_{15}H_{30}O_4$	ML
Trioxyethylene monododecyl ether	$C_{12}H_{25}(OCH_2CH_2)_3OH$	$C_{12}EO_3$

2.2 Methods

2.2.1 Visual observation

Appropriate ratio of water and surfactants were mixed well and kept at desired temperature for a long time in order to achieve equilibration. The solutions were observed by placing between crossed polarizers, in both still and shaken condition. The presence or absence of birefringence and flow-birefringence were carefully noted. This gives an idea of the nature of surfactant solution phases. However, for wormlike micelle characterization, we mainly depend on rheometry, as detailed below.

2.2.2 Rheometry[1-4]

The rheological behavior of structured fluids, polymer and surfactant solutions and suspensions is a most fascinating subject. The basic principle of rheology (derived from the greek word: rheos = river) is the correlation of the deformation of a fluid with the occurring stresses, in particularly during flowing processes. Rheology is the study of the deformation and flow of matter. In a gross sense, a rheological measurement tells one how "hard" or "soft" a material is, or it indicates how "fluid-like" or solid-like" it is. These characteristics of a material depend on the time scale it is probed. A rheometer measures the rheological properties of a complex fluid (such as solutions of surfactant or polymer) as a function of rate or frequency of deformation.

2.2.2.1 Basic Principle of Rheology:

2.2.2.1.1 Steady-Shear Rheology:

Simple steady-shear is the easiest flow to generate and is therefore, of central importance in rheology. Let us consider a fluid between two plates as shown in Figure 2.6. Suppose that both plates are initially at rest with no flow occurring. When a force F is applied to the upper plate, a shear stress σ is generated in the fluid from the cohesive forces between the fluid molecules. It is assumed that the gap h is small and strain is the same at all points. The shear is given by

$$\sigma = F/S \qquad (2-1)$$

where S is the surface area of upper face. Alternately, σ may be defined as the force that a flowing fluid exerts per unit area of its surface in a direction parallel to the flow. The rate of deformation or the shear rate is the first derivative of strain with respect to time.

$$\dot{\gamma} = \frac{d\gamma}{dt} = \frac{1}{h}\frac{da}{dt} \qquad (2\text{-}2)$$

A shear viscosity is defined as

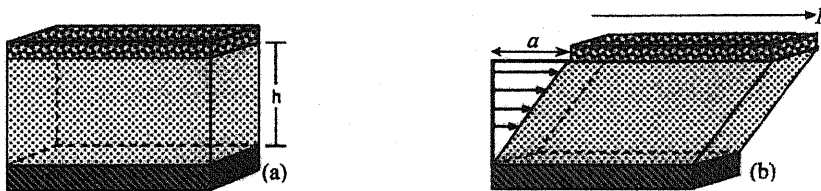$$\eta = \frac{\sigma}{\dot{\gamma}} \qquad (2\text{-}3)$$

Figure 2.1: Test fluid between two parallel plates separated by a gap h. Steady shear

(a/h) is applied to the fluid at rest (a) by sliding the upper plate at a constant velocity

given by da/dt (b).

Note that this expression is analogous to Newton's law for simple liquids and

the viscosity here is a function of shear rate and not a constant parameter.

Various kinds of flow curves, i.e., double logarithmic plots of viscosity versus

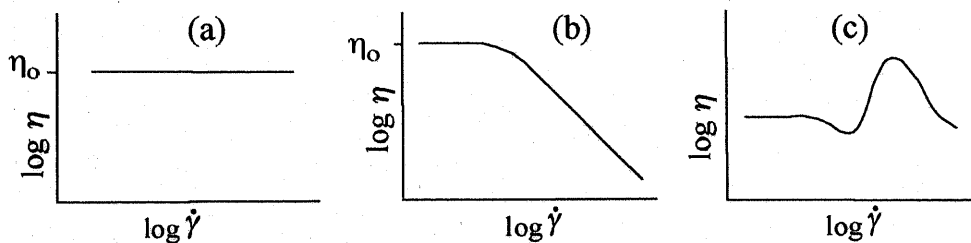shear –rate, observed in wormlike micellar systems are shown Figure 2.2.

Figure 2.2: Various types of flow curves shown by the solution of surfactant systems.

The simplest type of steady-shear response is Newtonian behavior, where the

viscosity is independent of the shear-rate [Figure 2.2(a)]. This is also manifested as a

linear relationship between shear stress and shear rate, with the slope of the line

24

defining the viscosity. Most low molecular-weight liquids and gases show Newtonian behavior. Among the non-Newtonian phenomena, the most widely observed in the viscoelastic micellar systems is shear thinning. In the simplest case, the sample shows Newtonian behavior at low shear rate and shear thinning at higher shear rate [Figure 2.2(b)]. The zero-shear viscosity may be obtained by the extrapolation of the viscosity curve to zero shear-rate. Since during the steady-shear experiment the sample is deformed extensively the microstructure of the material is disturbed. For such strong deformations, the theoretical aspects of the rheology of wormlike micellar solution is difficult. However, Cates and his collaborators have made some advance in this direction.[5, 6] They have extended the reptation model of living polymer to strong flow condition and predicted a critical shear rate and a plateau value in the stress versus shear-rate plot which have been experimentally observed. Shear thickening [Figure 2.2(c)], which corresponds to the increase in viscosity over a range of shear-rate, is observed much less frequently.

2.2.2.1.2 Dynamic (Oscillatory-Shear) Rheology:

In dynamic shear flow, a sinusoidally varying deformation (strain) is applied to the sample (Figure 2.3).

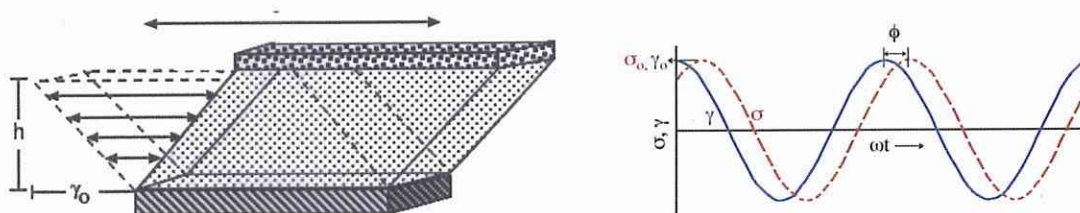$$\gamma = \gamma_o \sin (\omega t) \qquad (2\text{-}4)$$

Figure 2.3: Oscillatory deformation of the viscoelastic material and variation of strain (solid line) and stress (dotted line) with time.

25

where γ is strain –amplitude (i.e. the maximum applied deformation) and ω is the frequency of the oscillations. The shear stress generated by the oscillatory shear will again be sinusoidal but will be shifted by a phase angle (ϕ) with respect to the strain wave form:

$$\sigma = \sigma_o \sin(\omega t + \phi) \tag{2-5}$$

The presence of a phase angle term means that the maxima and minima of sinusoidally varying stress signals are not necessarily coincident with the maxima and minima in the strain. For perfect solid, stress is in phase with strain ($\phi = 0$). In case of purely viscous liquid, stress is in quadrature with strain ($\phi = \pi/2$). For viscoelastic materials ϕ has an intermediate value. At small strains and for a given viscoelastic material, the fluid structure is not much disturbed by the deformation and the stress measured during oscillatory deformation is controlled by the spontaneous rearrangements or relaxation. In this case, the shear stress produced by a small amplitude deformation is proportional to amplitude of the applied strain γ_0, and deformation ratio σ_o / γ_0 and the phase angle ϕ are the material properties at any frequency, which is the main feature of linear viscoelasticity.

Using trigonometric identities, the stress wave can be decomposed into two components, one in-phase with the strain and the other out-of–phase by 90 degrees:

$$\sigma = \sigma_o \cos(\phi) \sin(\omega t) + \sigma_o \sin(\phi) \cos(\omega t) \tag{2-6}$$

We can rewrite the above expression in terms of two material functions (G' and G'') as

$$\sigma = \gamma_o [G' \sin(\omega t) + G'' \cos(\omega t)] \tag{2-7}$$

$$\text{Elastic or storage modulus, } G' = (\sigma_o/\gamma_o) \cos\phi \tag{2-8}$$

$$\text{Viscous or loss modulus, } G'' = (\sigma_o/\gamma_o) \sin\phi \tag{2-9}$$

26

The elastic modulus (G'), which is related to the stress in phase with the imposed strain, provides information about the elastic nature of the material. Because elastic behavior implies the storage of deformational energy in the system, this parameter is also called the storage modulus. The viscous modulus (G''), on the other hand, is related to the stress component, which is completely out-of-phase with the displacement. This parameter characterizes the viscous nature of the material. Because viscous deformation results in the dissipation of energy, the G'' parameter is also called the loss modulus. A purely elastic material would exhibit a non-zero elastic modulus and a viscous $G' = 0$. In contrast, a purely viscous material would show a zero elastic modulus. A viscoelastic material will exhibit non-zero values for both G' and G''.

The complex viscosity ($|\eta^*|$) is defined as:

$$|\eta^*| = \frac{\left(G'^2 + G''^2\right)^{\frac{1}{2}}}{\omega} \tag{2-10}$$

The variation of complex viscosity with frequency is analogous to the variation of steady viscosity versus shear-rate.

The storage and loss moduli are given by:

$$G'(\omega) = \frac{G_0(\omega\tau)^2}{1+(\omega\tau)^2} \tag{2-11}$$

$$G''(\omega) = \frac{G_0(\omega\tau)}{1+(\omega\tau)^2} \tag{2-12}$$

It is possible to define and measure various other rheological functions besides $G^*(\omega) = G'(\omega) + iG''(\omega)$. For example:

a) The relaxation function $G(t)$ is defined as the ratio of the time-dependent stress to a suddenly applied strain held constant after application.

b) For the transient strain generated when a constant stress is applied at some point in time and then brought down to zero value at some later time, the ratio of the transient strain to the constant stress value is called the creep function $J(t)$.

c) The Fourier transform of the creep function is called the complex compliance $J^*(\omega)$.

d) A material usually possesses a distribution of retarded elastic response times $L(\tau)$ or viscous relaxation times $H(\tau)$.

However, when the material deformation is small, the experimental results lie in the linear viscoelastic region and all these functions are interchangeable as shown in Figure 2.4:
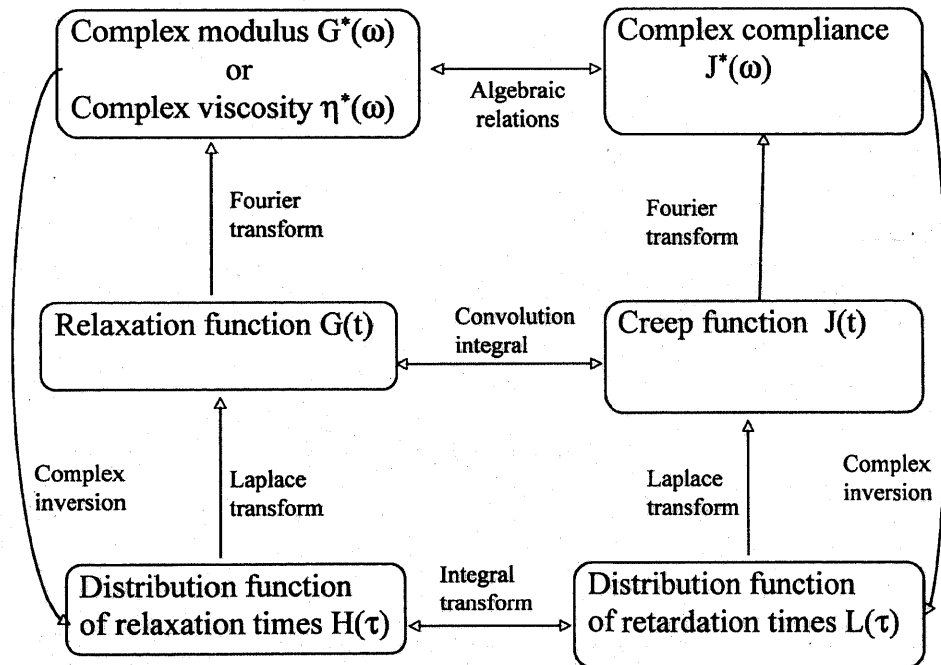

Figure 2.4: Interrelations between the various linear viscoelastic functions.

Thus all possible types of experiment yield the same information about the material.

2.2.2.2 Instrumentation

Rheological measurements are typically performed on a rheometer. There are several categories of rheometers, with the most prominent being capillary rheometer (which utilize pressure-driven or poiseuille flows) and rotational rheometers (which use drag flows). Capillary rheometers are capable of measuring only the steady-shear properties of a fluid, not the dynamic rheological properties. For this reason, we will focus solely on rotational instruments. Two types of rotational rheometers exist: stress-controlled rheometers and strain-controlled rheometers. In a strain-controlled rheometer, a known deformation (strain or shear rate) is applied to the fluid, and the stress is detected. Typically, the strain is applied by rotating one segment of the geometry, and a transducer connected to the other segment measures the stress. A stress rheometer operates in the opposite fashion, by applying a controlled stress and measuring the resulting deformation. In the past few years, stress rheometers have become immensely popular because of great sensitivity and wide torque range.

In rheological measurements, depending on the property of the test material, test conditions to be maintained and type of the material property to be studied, various geometries such as parallel-plates, cone-and- plate, concentric cylinders, can be used to impose shearing flow. Schematic diagrams of cone-plate and couette (concentric cylinders) geometries are shown in Figure 2.5. The parallel-plate and cone-plate geometries are common due to a small amount of sample required and ease to load and clean. The advantage of the cone-plate geometry over the parallel-plate one is that the small cone angle θ (<0.2rad) provides a uniform shear throughout the sample. Couette geometry is suitable for low-viscosity samples. Flow is generated in a rotational geometry by moving one of the systems in such a way that the fluid is dragged along the wall.
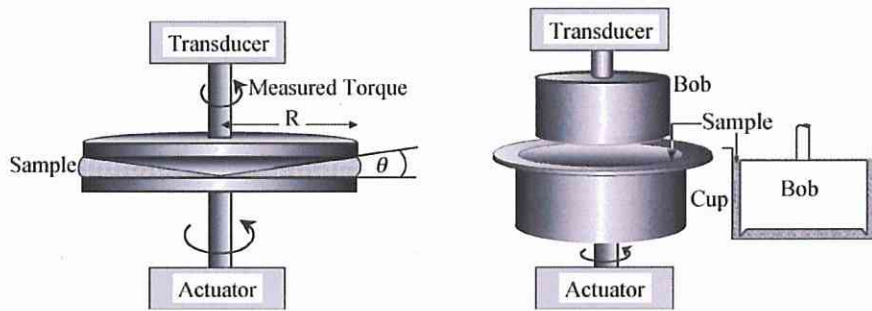
29

Figure 2.5: Schematic diagrams of cone-plate (left) and couette (right) geometries.

In a strain-controlled rheometer, input is the deformation and output is the torque. The raw data can be converted into rheologically significant quantities using the physical dimension of the geometry. On a cone-plate geometry with cone angle θ and radius of cone R, following equation relates the angular velocity Ω (rad.s^{-1}) of the lower plate induced by the actuator (as shown in Figure 2.5) to the shear-rate exerted on the sample:

$$\dot{\gamma} = \frac{\Omega}{\theta}$$

(2-13)

The response of the sample is measured by the transducer in terms of a torque (M), which is related to the shear-stress according to following relation:

$$\sigma = \frac{3M}{2\pi R^3}$$

(2-14)

The viscosity then can be obtained from equation (2-3). In a stress controlled rheometer, for the same geometry, a constant known stress is applied, and the angular displacement, ω, related to $\dot{\gamma}$ by $\Omega = d\omega/dt$ and equation (2-13), is measured. The viscosity then can be calculated from equation (2-3). This method is more sensitive, although at the price of higher instrument cost.

In oscillatory-shear measurement, the plate is made to oscillate from its mean position, with a maximum displacement up to an angle φ (in rad). The strain amplitude is then given by

$$\gamma_o = \frac{\varphi}{\theta} \qquad (2\text{-}15)$$

The response of the sample is in terms of sinusoidal torque (M) with a phase lag (ϕ) with respect to the input strain. The maximum stress amplitude (σ_o) is obtained from equation (2-14). The elastic and viscous moduli can then be calculated using equations (2-11) and (2-12), respectively. The final expressions are:

$$G' = \frac{3M\theta}{2\pi R^3 \varphi}\cos\phi \qquad (2\text{-}16)$$

$$G'' = \frac{3M\theta}{2\pi R^3 \varphi}\sin\phi \qquad (2\text{-}17)$$

References:

1. Larson, R.G. *The Structure and Rheology of Complex Fluids*, Oxford University Press, New York, **1999**.

2. Marin, G. *In Rheological Measurement* (Collyer, A. A.; Clegg, D. W.; Eds.), Chapman and Hall, UK, 2nd ed., **1998**.

3. Ferry, J.D. *Viscoelastic Properties of Polymers*, John Wiley & Sons, 3rd ed., **1980**.

4. Mezger, T.G. *The Rheology Handbook*, Curt R. Vincentz Verlag, Hannover, 2002

5. Cates, M.E. *J. Phys. Chem.* **1990**, *94*, 371

6. Spenley, N.A.; Cates, M.E.; McLeish, T.C.B. *Phys, Rev. Lett.* **1993**, *71*, 939

Chapter 3: Wormlike micelles in poly(oxyethylene) surfactant solution: Growth control through hydrophilic-group size variation

3.1 Introduction

Surfactants are now recognized to form long flexible micelles in aqueous solutions under the influence of various factors such as salt, temperature, cosurfactants etc.[1-5] These wormlike micelles, with linear polymer-like structure due to one-dimensional growth, can be highly viscoelastic like polymer solutions. Thus, these systems are very interesting from scientific and industrial standpoint. Therefore a large amount of research employing different materials and various techniques (such as rheology, cryo-TEM, light scattering, small-angle X-ray and neutron scattering etc.) have been carried out to characterize these systems.[2, 5-19] However, most of the past and recent work is focused on ionic surfactant systems.[20-25] Nonionic surfactants have comparatively lower CMC values than ionic ones,[26] allowing investigations through techniques and theories of dilute solutions. Their solution behavior is not complicated with electrostatic effects, which is the case with ionic surfactants.[6, 27, 28] Also, the size of the poly(oxyethylene) chain, the common head-group in many nonionic surfactants, can be varied easily. Therefore, wormlike micelles formed from poly(oxyethylene)-type nonionic surfactants may be easier to understand. Yet, there are few reports of formation of highly viscous (more than 1000 Pa·s) micellar solution with poly(oxyethylene)-type nonionic surfactants.

Recently, Acharya et al reported the formation of dilute viscoelastic micellar solutions in the nonionic poly(oxyethylene) cholesteryl ether (abbreviated as $ChEO_m$) surfactant systems and the maximum zero-shear viscosity reached about 3000 Pa·s.[29] Poly(oxyethylene) cholesteryl ether surfactants are unique nonionic surfactants in which the segregation tendency between the hydrophilic and hydrophobic groups is very strong compared with that of conventional alkyl ethoxylated surfactants and these surfactants are known to achieve

equilibrium interfacial conditions rather slowly due to the bulk and rigidity of the hydrophobic group.[30] As a remarkable fact, they form a liquid crystal in a pure state above their melting temperatures,[31] whereas conventional nonionic surfactants become simple liquids above the melting temperature. In dilute aqueous solutions of poly(oxyethylene) cholesteryl ether surfactants spherical micelles are formed at room temperatures[32] and increase in temperature promotes unidimensional micellar growth.[33] These surfactants, in binary systems and with cosurfactants, show interesting phase behavior, in which a rectangular phase or a defected lamellar phase in addition to conventional liquid crystals appear.[32, 34]

Several reports on mixed nonionic viscoelastic systems followed the publication of Ref. 29.[35-38] An important technique of such research has been the utilization of suitable hydrophobic amphiphiles as cosurfactants to promote unidimensional micellar growth. The effect of changing cosurfactant head-group size or hydrophobic tail length on micellar growth was investigated.[35-38] The increase in the hydrophobic alkyl chain of the cosurfactant or the decrease in the number of ethyleneoxide units in the head group of the cosurfactant decreased the fraction of cosurfactant required for inducing micellar growth.[16, 29, 35, 36] However, the effect of changing the head-group size of the hydrophilic surfactant over an extensively large range of sizes was not investigated.

In this study, we report the formation of wormlike micelles in solutions of poly(oxyethylene) cholesteryl ether surfactants with head-groups of exceedingly different sizes (ChEO$_m$, m = 15 and 30). We have used monolaurin and triethyleneglycol dodecyl ether as cosurfactants because they are known to induce one-dimensional micellar growth in several systems.[35, 36, 38] We present the rheological data of the systems and discuss the data in the light of current theories of viscoelasticity of wormlike micellar systems. We find our

results in agreement with the established concept of micellar growth due to the reduction of effective area per molecule in surfactant assembly.

3.2. Experimental

3.2.1 Materials

Poly(oxyethylene) cholesteryl ether (abbreviated as $ChEO_m$, m = 15 and 30) was purchased from Nihon Emulsion Co., Japan. Monolaurin (98%) was supplied by Tokyo Kasei Kogyo Co. Ltd. (Japan). Triethyleneglycol dodecyl ether ($C_{12}EO_3$) was obtained from Nikko Chemicals Co., Japan. All these chemicals were used as received. Millipore-filtered water was used to prepare all the samples.

☐

3.2.2 Methods

3.2.2.1 Observation of micellar transformation

Different ratios of the selected surfactants were dissolved in water by mixing well using magnetic stirrer. The samples were equilibrated for long times at 25 °C. They were observed between crossed polarizers. High viscosity, ability to trap bubbles for long times and shear birefringence was taken to be indication for the formation of long micelles due to unidimensional micellar growth.

3.2.2.2 Rheological Measurement

Samples for rheological measurements were prepared by adding the required amount of $C_{12}EO_3$ and monolaurin to measured volumes of aqueous $ChEO_m$ solution of a desired concentration. The samples were homogenized and kept in a water bath at 25 °C for at least 48 hours to ensure equilibration before performing measurements. Rheological measurements

were performed in a stress-controlled rheometer, AR-G2 (TA instruments co.), using cone-plate geometry modified with a solvent-trap to minimize evaporation and with the plate temperature controlled by a peltier unit. Frequency sweep measurements were performed in the linear viscoelastic regime of the samples, as determined previously by dynamic strain sweep measurements.

3.3.Results

3.3.1 Steady shear rheology

Steady-state shear-rate viscosity plots for the aqueous 0.06 M (excluding cosurfactant) $ChEO_{30}$ systems containing various $C_{12}EO_3$ ratios are shown in Figure 3.1. At low $C_{12}EO_3$ mixing fraction (up to $X \approx 0.4$), the viscosity is very low and is independent of
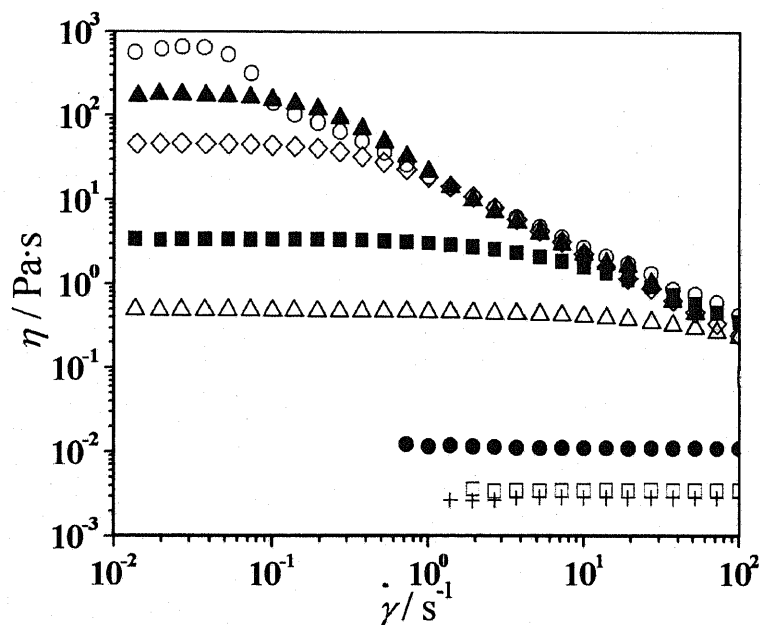

Figure 3.1 Steady-shear-rate viscosity plots of the 0.06 M (excluding cosurfactant) $ChEO_{30}$ solutions at 25 °C with different mixing fractions of $C_{12}EO_3$. (O) X = 0.76, (▲) X = 0.74, (◇) X = 0.73, (■) X = 0.72, (△) X = 0.71, (●) X = 0.66, (□) X = 0.34, (+) X = 0.
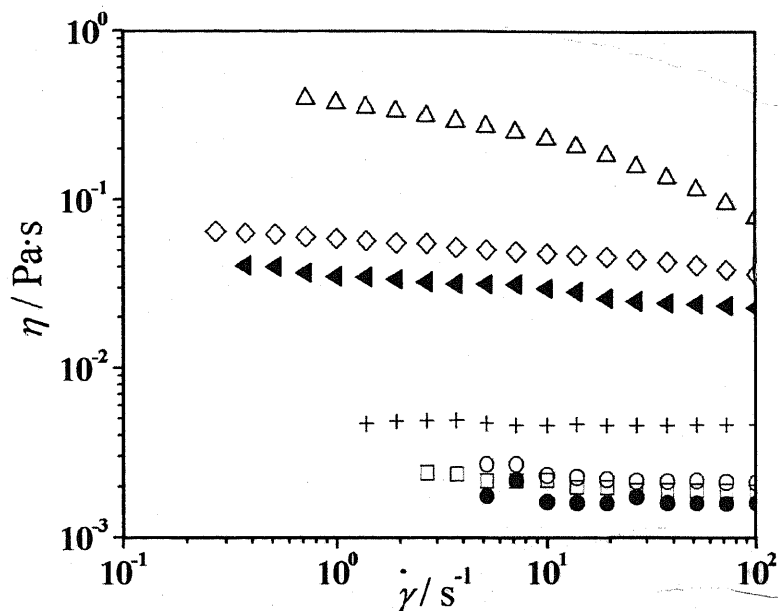
35

Figure 3.2   Steady-shear-rate viscosity data of the 0.06M (excluding cosurfactant) $ChEO_{15}$ systems with different concentrations of monolaurin at 25 °C. Legends: ($\triangle$) X = 0.53, ($\diamondsuit$) X = 0.51, ($\blacktriangleleft$) X = 0.5, (+) X = 0.47, (O) X = 0.44, ($\square$) X = 0.39, ($\bullet$) X = 0.

shear at low shear rate (Newtonian fluid). At $X \approx 0.65$ and above, however, the Newtonian behavior is limited to low shear rate, which can be taken as evidence of the formation of long wormlike micelles. At high concentration ($X \approx 0.74$ and above) samples are viscoelastic with large low -shear viscosity values.

Steady shear measurements were carried out on 0.06 M (excluding cosurfactant) $ChEO_m$ systems (m = 15, 30) containing monolaurin. The data is presented in Figure 3.2. The $ChEO_{15}$ solution low-shear viscosity does not increase significantly with increasing mole fraction of monolaurin up to about $X = 0.4$. For higher mole fractions viscosity increases with successive increase of X up to phase separation at about $X = 0.55$. These higher mole-fraction systems also manifest slight shear-thinning behavior. The maximum viscosity obtained is not very high (~1 Pa·s). The solutions with higher X were shear birefringent, indicating unidimensional micellar growth. In the case of $ChEO_{30}$ solutions no shear birefringent

systems were obtained upon monolaurin addition and steady shear measurements revealed

insignificant increase in viscosity upon successive increase in monolaurin content (Figure 3.3).

At $X \approx 0.5$ phase separation occurs. These results are discussed further below.
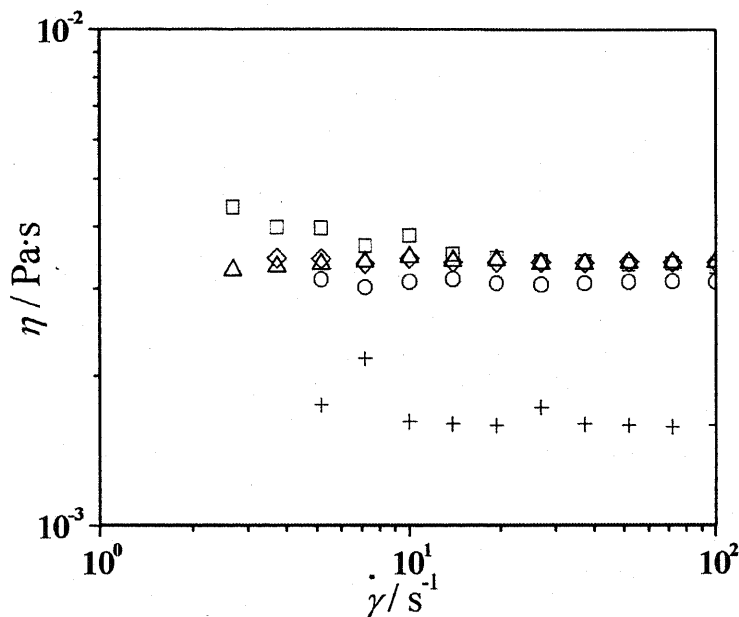

Figure 3.3 Steady-shear-rate viscosity data of the 0.06 M (excluding cosurfactant) $ChEO_{30}$

systems with different concentrations of monolaurin at 25 °C. Legends: (+) X = 0, (O) X =

0.3, (□) X = 0.39, (◇) X = 0.45, (△) X = 0.5.

3.3.2 Dynamic rheology

To study the viscoelastic properties of the wormlike micellar solutions in the

$ChEO_{30}$-$C_{12}EO_3$ systems, oscillatory shear measurements have been performed. Figure 3.4

shows the variation of the elastic or storage modulus (G') and the viscous or loss modulus

(G'') with oscillation frequency at $C_{12}EO_3$ concentrations of $X = 0.74 - 0.77$. In these systems,

liquidlike behavior ($G' < G''$) is observed in the low-frequency region, but both G' and G''

increase with ω and viscoelastic behavior ($G' > G''$) is observed in the high-frequency region.

As can be seen from Figure 3.4 with increasing concentration of $C_{12}EO_3$ the region of $G' > G''$

extends to lower frequency, and above $X \approx 0.74$ of $C_{12}EO_3$, the system is viscoelastic in a wide range of shear frequency and has a rheological pattern typical of entangled wormlike micelles. The rheological data on 0.06 M $ChEO_{15}$-$C_{12}EO_3$ systems have been published in Ref. 29.
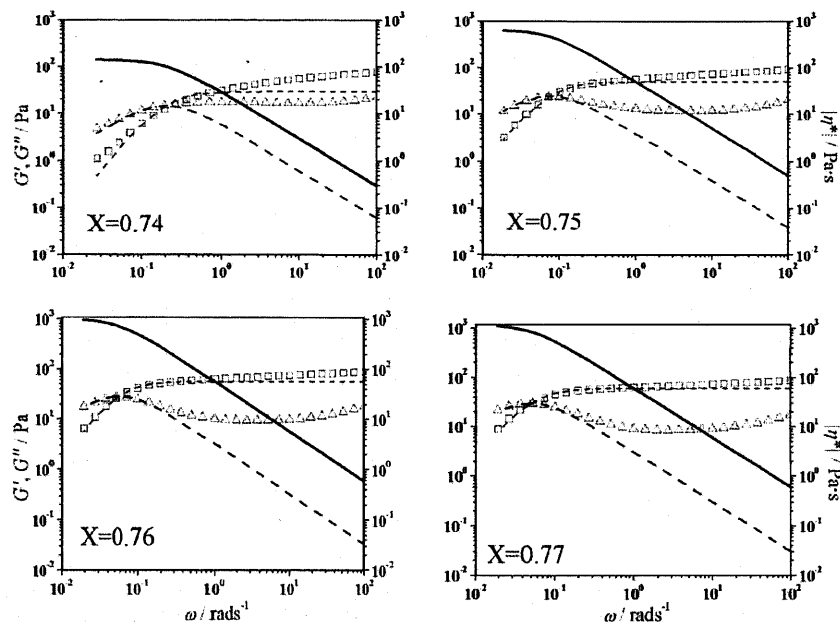

Figure 3.4 Variation of G', G'' and $|\eta^*|$ as a function of ω for the $C_{12}EO_3$ containing 0.06 M (excluding cosurfactant) $ChEO_{30}$ solution systems at 25 °C for different $C_{12}EO_3$ concentrations. Legends: ($\square$) G' experimental, ($\triangle$) G'' experimental, (--) Maxwell model, (—) complex viscosity.

The η_0 values for the Newtonian systems of low viscosity have been obtained by extrapolating the viscosity to zero-shear rate. For viscoelastic systems following Maxwellian behavior at low-shear frequency, η_0 values were estimated from the following equation:

$$\eta_0 = G_0 \tau \qquad (3\text{-}1)$$

Alternately, the following relationship allows one to estimate η_0 by extrapolating the complex viscosity values ($|\eta^*|$) to zero shear frequency:

$$|\eta^*| = \frac{\left(G'^2 + G''^2\right)^{1/2}}{\omega} = \frac{\eta_0}{\sqrt{1 + \omega^2 \tau^2}} \tag{3-2}$$

The values of viscoelastic samples obtained from the estimated values of G_0 and τ are only approximate values. The zero-shear viscosity values of the different systems are plotted in Figure 3.5 below.

Figure 3.5 Variation of zero-shear viscosity of 0.06 M (excluding cosurfactant) $ChEO_m$-cosurfactant (m = 15 and 30, cosurfactants: monolaurin or $C_{12}EO_3$) systems as a function of cosurfactant mole fraction at 25 °C.

3.4. Discussion

3.4.1 Effect of cosurfactant type

In the $ChEO_{15}$-monolaurin and the $ChEO_{15}$-$C_{12}EO_3$ systems up to about $X = 0.45$ the zero-shear viscosities do not change with increasing cosurfactant mixing fractions and the viscosity values for the two systems are almost indistinguishable for the same cosurfactant mixing fractions. The steady-shear viscosity measurement of these systems (Figure 3.2) reveals shear-independent viscosities for $X = 0 \sim 0.47$ and therefore no micellar growth. With increasing mixing fractions, slight growth followed by phase-separation occurs in the case of monolaurin and highly viscoelastic solutions are formed in the case of $C_{12}EO_3$. However, the growth trend in both systems is almost the same. Thus, in this case, the effectiveness of monolaurin and $C_{12}EO_3$ cannot be conclusively compared.

In the case of the $ChEO_{30}$-monolaurin and the $ChEO_{30}$-$C_{12}EO_3$ systems also, we cannot compare the effectiveness of the cosurfactants due to the phase separation in the $ChEO_{30}$-monolaurin system at about $X = 0.5$. We note, however, that up to this mixing fraction ($X = 0.5$) the viscosities of the two systems are almost constant and identical.

3.4.2 Effect of the hydrophilic surfactant headgroup size

In the $ChEO_m$-$C_{12}EO_3$ systems highly viscoelastic solutions are formed with large cosurfactant mole fractions. The viscoelastic behavior of the entangled micelles is described by the Cates model,[5, 39] which considers two processes of stress relaxation – reptation or the reptile-like motion of the micelle along a tube and the reversible scission of micelles – taking place on two time scales, namely, the reptation time τ_{rep} and the breaking time τ_b. The viscoelastic behavior of such a system at low shear frequency often follows the Maxwell model of viscoelastic fluids with a single relaxation time τ given by $(\tau_b.\tau_{rep})^{1/2}$ and plateau modulus (G_0) described by equations 3-3 and 3-4[40]:

$$G'(\omega) = \frac{\omega^2\tau^2}{1+\omega^2\tau^2}G_0 \qquad (3\text{-}3)$$

$$G''(\omega) = \frac{\omega\tau}{1+\omega^2\tau^2}G_0 \qquad (3\text{-}4)$$

G'' does not show a clear minimum, but a very wide one followed by an upturn with increasing ω, suggesting a wide spectrum of the stress relaxation at high frequency or several relaxation processes superimposed.

The analysis of the oscillatory-shear measurement data reveals that in the maximum viscosity region ($X \approx 0.77$) of the 0.06 M (excluding cosurfactant) $ChEO_{30}$-$C_{12}EO_3$ the G_0 value is higher than that in the maximum viscosity region of the 0.06 M (excluding cosurfactant) $ChEO_{15}$-$C_{12}EO_3$.[29] G_0 is related to the average length between entanglements, l_e (nanometers), in the network by the equation[41] $G_0 \approx kT/(l_e^{9/5})$, a larger value of G_0 in the $ChEO_{30}$-$C_{12}EO_3$ system corresponds to a smaller l_e, that is, a smaller mesh size of the transient network that is probably due to a higher total surfactant content in the $ChEO_{30}$-$C_{12}EO_3$ system. However the relaxation time in the $ChEO_{30}$-$C_{12}EO_3$ system in the maximum viscosity region is smaller than that in the $ChEO_{15}$-$C_{12}EO_3$ system, implying faster stress relaxation. Similarly, it can be seen that the ratio G''_{min}/G_0 in the system $ChEO_{30}$-$C_{12}EO_3$ (~ 0.14) is higher than that in the system

ChEO$_{15}$-C$_{12}$EO$_3$ (~0.03 at X = 0.62)[29] in the maximum viscosity region. Because the quantity

is related to the micellar contour length L through the following relation when τ_b is much

longer than the Rouse time, (τ_R)[42,39].

$$G''_{min}/G_0 \approx l_e/L \qquad (3\text{-}5)$$

The larger G''_{min}/G_0 and smaller l_e in ChEO$_{30}$-C$_{12}$EO$_3$ suggest significantly smaller L. On the

basis of Doi-Edwards relation,[43] $\tau_{rep} \propto L^3 \phi^{3/2}$, where ϕ is the volume fraction of surfactant, it

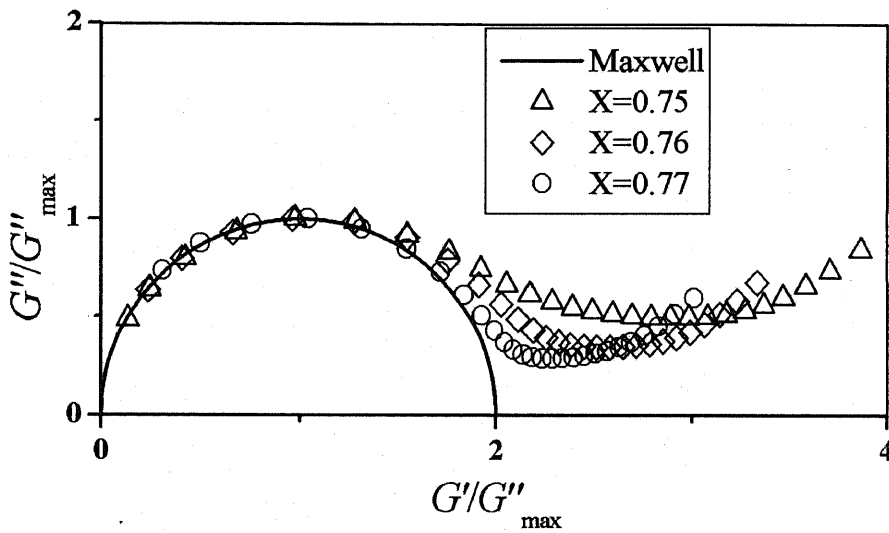can be assumed that the micelles with shorter contour lengths require shorter times to reptate

Figure 3.6 Normalized Cole-Cole plots for 0.06 M (excluding cosurfactant) ChEO$_{30}$-C$_{12}$EO$_3$ systems at 25 °C for various mixing fractions of C$_{12}$EO$_3$. X denotes the cosurfactant mixing fraction.

and therefore can undergo stress relaxation quickly. Also the Doi-Edwards[43] relation $G_0 \propto$

$\phi^{3/2}/L$, implies an increase in G_0 with a decrease in L probably because decrease in L at a

value of ϕ would increase the number of micelles and consequently the number density of

micelles in the system. Such theoretical predictions are consistent with the rheological results

of the ChEO$_{30}$-C$_{12}$EO$_3$ and ChEO$_{15}$-C$_{12}$EO$_3$ systems in maximum viscosity regions. These

results imply that upon decreasing the EO chain length of ChEO$_m$ in the ChEO$_m$-C$_{12}$EO$_3$

system the average micellar length increases or micellar growth is favored.

41

Plots of G''/G''_{max} against G'/G''_{max} for $ChEO_{30}$-$C_{12}EO_3$ systems at different cosurfactant mixing fractions are shown in Figure 3.6. In this plot, known as normalized Cole-Cole plot,[44] a Maxwell material is characterized by a semicircle centered at $G'(\omega)/G''_{max} = 1$. It can be seen from the Figure 3.6 that with increasing $C_{12}EO_3$ concentration the system approaches Maxwellian behavior.
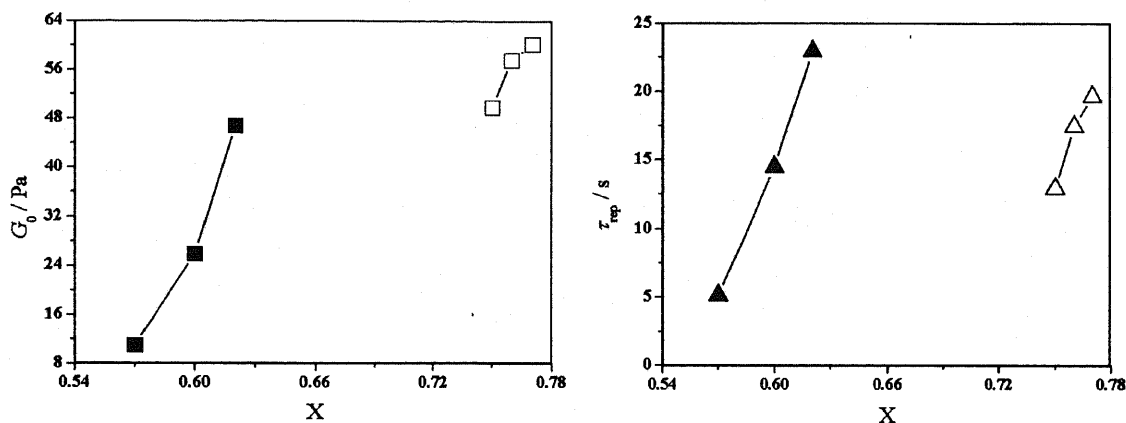

Figure 3.7 Variation of plateau modulus and relaxation time for 0.06 M (excluding cosurfactant) $ChEO_{30}$-$C_{12}EO_3$ system and $ChEO_{15}$-$C_{12}EO_3$ system at 25 °C with the mixing fraction of $C_{12}EO_3$ (X). Legends: open symbols: $ChEO_{30}$-$C_{12}EO_3$ system; closed symbols: $ChEO_{15}$-$C_{12}EO_3$ system.

From Figure 3.7 we see that both the plateau modulus and the relaxation time of the $ChEO_{30}$-$C_{12}EO_3$ system increases monotonously with cosurfactant ratio near the maximum viscosity composition range ($X \approx 0.74$–0.77). Since G_0 is usually proportional to the number density of the micellar aggregates, and therefore, reflects the mesh size of the network,[41] the increase in plateau modulus G_0 with concentration corresponds to the increase in the degree of entanglements. The increase in τ_{rep} reflects the one-dimensional growth of micelles with increasing concentration. This analysis corroborates the ideas of micellar growth previously

expressed from the discussion of steady-shear rheological data. Similar behavior is observed in the $ChEO_{15}$-$C_{12}EO_3$ system ($X \approx 0.59$-0.61).

The maximum value of the zero-shear viscosity, which is a product of the plateau modulus and the relaxation time (equation 3.1), in the $ChEO_{15}$-$C_{12}EO_3$ and the $ChEO_{30}$-$C_{12}EO_3$ systems are of the same order of magnitude. We observe that the plateau modulus is higher in the $ChEO_{30}$-$C_{12}EO_3$ system ($X = 0.77$) than that in the $ChEO_{15}$-$C_{12}EO_3$ system ($X = 0.62$) whereas the relaxation time is lower in the $ChEO_{30}$-$C_{12}EO_3$ system than that in the $ChEO_{15}$-$C_{12}EO_3$ system (Figure 3.7), and these opposite effects compensate each other, resulting in zero-shear viscosities of the same order of magnitude. The physical origin of these differences has been discussed previously.

In order to achieve viscosity of the same order of magnitude, higher mole fraction of cosurfactant is required in the $ChEO_{30}$-$C_{12}EO_3$ system ($X = 0.77$) than that in the $ChEO_{15}$-$C_{12}EO_3$ system ($X = 0.62$) (Figure 3.5). This can be understood from considerations of the curvature of the mixed surfactant layer. Incorporation of a cosurfactant with a small head-group reduces the effective area per molecule, which results in a decrease in the interfacial curvature of the surfactant self-assembly, thus leading to micellar growth.[1] In agreement with this concept, it has already been found that for any particular hydrophilic surfactant, the cosurfactant with the smaller head-group is the more effective for inducing micellar growth.[29,16] Also, for homologous hydrophilic surfactants in a small range of head-group sizes, it was previously found that less cosurfactant is required to induce micellar growth, i.e. reduce the effective area per molecule, in the case of the hydrophilic surfactant with the smaller head-group.[29] Our current investigations imply that the same concept is valid for a much wider range of head-group sizes.

In the monolaurin-$ChEO_{15}$ and monolaurin-$ChEO_{30}$ systems phase separation occurs without significant growth. In the first system only slight micellar growth is observed

before a liquid crystalline phase is formed. In the second system no growth occurs before a solid phase separates. This variation is again due to the difference in the head group size of the hydrophilic surfactants. In particular, the solid phase separation in the system can be attributed to the large difference of hydrophilicities of monolaurin and $ChEO_{30}$, which is known to cause phase separation in other systems.[37]

3.5 Conclusion

We make the first report of formation of highly viscous ($\sim 10^3$ Pa·s) wormlike micellar solution of long poly(oxyethylene) chain nonionic surfactant ($ChEO_{30}$) by adding appropriate hydrophobic cosurfactant. Such solutions manifest viscoelastic behavior at low net surfactant concentrations, i.e., in these systems steady-state shear-rate sweep measurements reveal shear-thinning and dynamic frequency sweep rheometry shows cross-over characteristic of Maxwell model. Such data agree with the concepts of entangled network structure and reptation in Cates' theory of living polymer. Similar data from solutions of the homologous series of hydrophilic surfactant $ChEO_m$ (m = 15 and 30) with $C_{12}EO_3$ cosurfactant demonstrate that the larger the head-group of the hydrophilic surfactant the more cosurfactant is required to induce elongation of micelles. Independent determination of the plateau modulus and relaxation time from the dynamic rheological data confirms the formation of longer micelles in the solution of the hydrophilic surfactant with the smaller head-group in the maximum viscosity compositions. We do not know of any published results that compare micellar growth for such a large range of head-group size of hydrophilic surfactant. Previous studies demonstrated the positive effect of reducing the head-group size in a limited range or of increasing the hydrophobic tail length of the cosurfactant on micellar growth.[35-38] Our current findings extend such results in the sense that now we can greatly vary the micellar length by selecting the size of the head-group of the hydrophilic surfactant and packing

44

constraints in micelles can be tuned by changing the head-group size of the hydrophilic surfactant as well as by varying the cosurfactant head or tail group sizes. We have also used monolaurin as cosurfactant in $ChEO_m$ solutions and found that phase separation occurs before significant micellar growth occurs. However, the trend is the same as that found with $C_{12}EO_3$. Therefore, although in other systems monolaurin was found to be a more effective cosurfactant than $C_{12}EO_3$, our present results indicate that phase separation can complicate the comparison of cosurfactant effectiveness and the outcome depends on the nature of the hydrophilic surfactant. We thus have a large range of head-group sizes of the surfactant as well as cosurfactant type at our disposal as a tool for control of micellar growth. New experiments may be devised based on such techniques. For example, since the nonionic systems of our study are free from electrostatic interactions, they can be profitably investigated utilizing recent developments in neutron scattering[45] and atomistic simulation.[46] Such research may provide deeper understanding of the elusive flexibility of wormlike micelles as well as bring out improvements for the computational aspects of colloid and interface science.

References

[1] C. A. Dreiss, Soft Matter 3 (2007) 956-970.

[2] L. J. Magid, J. Phys. Chem. B 102 (1998) 4064-4074.

[3] D. P. Acharya, H. Kunieda, in: P. Somasundaram, (Ed.), Encyclopedia of Colloid & Interface Science, 2nd ed., Dekker, 2006, pp. 6635-6651.

[4] D. P. Acharya, H. Kunieda, Adv. Colloid Interface Sci. 123-126 (2006) 401-413.

[5] M. E. Cates, S. J. Candau, J. Phys. Condens. Matter 2 (1992) 6869-6892.

[6] R. G. Shrestha, L. K. Shrestha, K. Aramaki, J. Colloid Interface Sci. 311 (2007) 276-284.

[7] D. Varade, C. Rodriguez, L. K. Shrestha, K. Aramaki, J. Phys. Chem. B 111 (2007) 10438-10447.

[8] W. Chen, P. D. Butler, L. J. Magid, Langmuir 22 (2006) 6539-6548.

[9] P. Schurtenberger, C. Cavaco, Langmuir 10 (1994) 100-108.

[10] B. A. Schubert, E. W. Kaler, N. J. Wagner, Langmuir 19 (2003) 4079-4089.

[11] T. Shikata, S. Imai, Y. Morishima, Langmuir 13 (1997) 5229-5234.

[12] J. Berret, Langmuir 13 (1997) 2227-2234.

[13] H. Kunieda, C. Rodriguez, Y. Tanaka, M. H. Kabir, M. Ishitobi, Colloids and Surf. B 38 (2004) 127-130.

[14] C. Rodriguez, K. Hattori, D. P. Acharya, T. Sakai, H. Kunieda, Langmuir 19 (2003) 8692-8696.

[15] S. Engelskirchen, D. P. Acharya, M. Garcia-Roman, H. Kunieda, Colloids and Surf.A 279 (2006) 113-120.

[16] C. Rodriguez, D. P. Acharya, A. Maestro, K. Hattori, H. Kunieda, J. Chem. Eng. Soc. Jpn. 37 (2004) 622-629.

[17] D. P. Acharya, H. Kunieda, Y. Shiba, K. Aratani, J. Phys. Chem. B 108 (2004) 1790-1797.

[18] T. Sato, D. P. Acharya, M. Kaneko, K. Aramaki, Y. Singh, M. Ishitobi, H. Kunieda, J. Disp. Sci. Tech. 27 (2006) 611-616.

[19] Z. Lin, Langmuir 12 (1996) 1729-1737.

[20] L. S. C. Wan, J. Pharm. Sci. 55 (1966) 1395.

[21] S. Gravsholt, J. Colloid Interface Sci. 57 (1976) 575.

[22] A. Khatory, F. Kern, F. Lequeux, J. Appell, G. Porte, N. Morie, A. Ott, W. Urbach, Langmuir, 9 (1993) 933-939.

[23] T. Imae, S. Ikeda, J. Phys. Chem. 90 (1986) 10030.

[24]□ D. P. Acharya, K. Hattori, T. Sakai, H. Kunieda, Langmuir 19 (2003) 9173-9178.

[25]□ D. P. Acharya, T. Sato, M. Kaneko, Y. Singh, H. Kunieda, J. Phys. Chem. B 110 (2006) 754-760.

[26]□ M. J. Rosen, Surfactants and Interfacial Phenomena; John Wiley and Sons Inc.: New York, 1989; Chapter 3.

[27]□ S. Safran, P. Pincus, M. E. Cates, F. Mackintosh, J. Phys. (Paris) 51 (1990) 503.

[28]□ F. Mackintosh, S. Safran, P. Pincus, Europhys. Lett. 12 (1990) 697.

[29]□ D. P. Acharya, H. Kunieda, J. Phys. Chem. B 107 (2003) 10168-10175.

[30]□ K. Holmberg, B. Jönsson, B. Kronberg, B. Lindman, Surfactants and Polymers in Aqueous Solution; 2ed; Wiley: New York, 2002; Chapter 1.

[31]□ M. A. López-Quintela, A. Akahane, C. Rodríguez, H. Kunieda, J. Colloid Interface Sci. 247 (2002) 186-192.

[32]□ T. Sato, M. K. Hossain, D. P. Acharya, O. Glatter, A. Chiba, H. Kunieda, J. Phys. Chem. B 108 (2004) 12927-12939.

[33]□ C. Moitzi, N. Freiberger, O. Glatter, J. Phys. Chem. B 109 (2005) 16161-16168.

[34]□ M. K. Hossain, D. P. Acharya, T. Sakai, H. Kunieda, J. Colloid Interface Sci. 277 (2004) 235-242.

[35]□ A. Maestro, D. P. Acharya, H. Furukawa, J. M. Gutierrez, M. A. Lopez-Quintela, M. Ishitobi, H. Kunieda, J. Phys. Chem. B 108 (2004) 14009-14016.

[36]□ D. Varade, K. Ushiyama, L. K. Shrestha, K. Aramaki, J. Colloid Interface Sci. 312 (2007) 489-497.

[37]□ D. P. Acharya, M. K. Hossain, J. Feng, T. Sakai, H. Kunieda, Phys. Chem. Chem. Phys. 6 (2004) 1627-1631.

[38]□ C. Rodriguez, K. Aramaki, Y. Tanaka, M. A. Lopez-Quintela, H. Kunieda, J. Colloid Interface Sci. 291 (2005) 560-569.

[39] R. Granek, M. E. Cates, J. Chem. Phys. 96 (1992) 4758-4767.

[40] R. G. Larson, The Structure and Rheology of Complex Fluids; Oxford University

Press: New York, 1999; Chapter 12.

[41] H. Rehage, H. Hoffmann, J. Phys. Chem. 92 (1988) 4712-4719.

[42] J. F. A. Soltero, J. E. Puig, O. Manero, Langmuir 12 (1996) 2654-2662.

[43] F. Kern, F. Lequeux, R. Zana, S. J. Candau, Langmuir 10 (1998) 1714-1723.

[44] P. A. Hassan, S. J. Candau, F. Kern, C. Manohar, Langmuir 14 (1998) 6025-6029.

[45] W.-R. Chen, P. D. Butler, L. J. Magid, Langmuir 22 (2006) 6539-6548

[46] E. S. Boek, W. K. den Otter, W. J. Briels, D. Iakovlev, Phil. Trans. R. Soc. London A

362 (2004) 1625-1638

Chapter 4: Temperature sensitivity of wormlike micelles in poly(oxyethylene) surfactant solution: importance of hydrophilic-group size

4.1 Introduction

Surfactant molecules can self-assemble in dilute aqueous solution to form aggregates greatly extended in one dimension.[1-5] Such growth can occur due to the addition of electrolytes, hydrophobic cosurfactants, polar oils or even in binary systems with increasing concentration of surfactant.[6-19] All these factors reduce the spontaneous curvature of the surfactant self-assembly and cylindrical geometry becomes more stable with respect to the more curved spherical geometry. When the contour length of such aggregates exceeds a certain length called the persistence length, their structure and dynamics resemble those of flexible polymers in solution, and are described as wormlike micelles.[20, 21] Lattice statistical theories (e.g. mean-field theory) originally developed for polymer solutions have been adapted to describe the equilibria of these systems.[21, 22] Similarly, application of the reptation theory of polymer solution has helped explain the dynamics of these systems, in particular the power law dependence of viscoelastic relaxation time on the length of micelles.[23-25]

The mean-field theory equilibrium description mentioned above predicts an average micelle contour length that decreases exponentially with increasing temperature if there does not exist any other factor that modifies this behavior.[21] In poly(oxyethylene) surfactants, the average curvature reduction of the surfactant layer due to the dehydration of the head-group with increasing temperature is a potential mechanism favoring temperature induced micellar growth.[26-28] For micelles of short poly(oxyethylene) chain surfactants, some studies reveal that the temperature induced curvature reduction can be strong enough for the high viscosity compositions to encourage the formation of three-fold junctions with local negative curvature.[10, 16]

This effect reduces the viscosity with increasing temperature. In the case of the lower viscosity compositions, viscosity was found to increase with temperature, indicating micellar growth. Whatever the case, it can be concluded that the reduction of the average curvature of micellar interface with temperature can overcome the thermal stabilization of micellar end-caps.

The rheological properties of wormlike micellar solution formed in water/Tween-80/$C_{14}EO_3$ system were found to be considerably temperature-sensitive.[11] The hydrophilic head-group of Tween-80 contains a large number of poly(oxyethylene) groups. However, the head-group is branched and there are no known data on similar systems to compare and conclude on the effect of head-group size variation on the temperature sensitivity of poly(oxyethylene) surfactants.

Poly(oxyethylene) cholesteryl ether ($ChEO_m$) surfactants are remarkable in that they form highly viscous micellar solutions when appropriate cosurfactants are added in aqueous or mixed solvents.[13, 17, 29] In chapter 3, we discussed the formation of viscoelastic wormlike micellar solutions of poly(oxyethylene) cholesteryl ether surfactant having large head-group (30 ethylene oxide units).[30] This result opens up the possibility of studying the variation of temperature sensitivity of poly(oxyethylene) surfactant wormlike micelles through changing the chain length of the poly(oxyethylene) head-group over a large range.

Therefore we have proceeded with the investigation of the temperature sensitivity of the rheology of the $ChEO_m$ (m = 15, 30) micellar systems containing $C_{12}EO_3$ and monolaurin cosurfactant, the same surfactants studied in chapter 3. We report our findings in this presentation. We have performed rheological measurements on the several systems. We present the data and the analysis and discuss the results by comparing with other complementary researches.

4.2 Experimental

4.2.1 Materials

Poly(oxyethylene) cholesteryl ether (abbreviated as $ChEO_m$, m = 15 and 30) was purchased from Nihon Emulsion Co., Japan. Monolaurin (98%) was supplied by Tokyo Kasei Kogyo Co. Ltd. (Japan). Triethyleneglycol dodecyl ether ($C_{12}EO_3$) was obtained from Nikko Chemicals Co., Japan. All these chemicals were used as received. Millipore-filtered water was used to prepare all the samples.

☐

4.2.2 Methods

4.2.2.1 Observation of micellar transformation

Different ratios of the selected surfactants were dissolved in water by mixing well using magnetic stirrer. The samples were equilibrated for long times at 15, 20, 25, 30, 35, 40 and 45 °C. They were observed between crossed polarizers. Birefringence of samples at rest and in shaken condition was carefully noted at different temperatures.

4.2.2.2 Rheological Measurement

Samples for rheological measurements were prepared by adding the required amount of $C_{12}EO_3$ and monolaurin to measured volumes of aqueous 0.06 M $ChEO_m$ solutions. The samples were homogenized and kept in a water bath at some set temperature (15, 20, 25, 30, 35, 40, 45 °C) for at least 48 hours to ensure equilibration before performing measurements. Rheological measurements were performed in a stress-controlled rheometer, AR-G2 (TA instruments co.), using cone-plate geometry modified with a solvent-trap to minimize evaporation and with the plate temperature controlled by a peltier unit. Frequency sweep measurements were performed in the

linear viscoelastic regime of the samples, as determined previously by dynamic strain sweep measurements.

4.3 Results

4.3.1 Steady shear rheology

Steady-state shear-rate viscosity data for the aqueous 0.06 M (excluding cosurfactant) $ChEO_{30}$ and $ChEO_{15}$ systems containing various monolaurin and $C_{12}EO_3$ ratios at 25 °C have been presented in chapter 3. We have performed steady-shear rheometry on the same systems at various temperatures. The monolaurin containing systems could not be measured at low temperatures because the cosurfactant phase separates as solid. Also, for systems containing large amount of $C_{12}EO_3$ the cloud
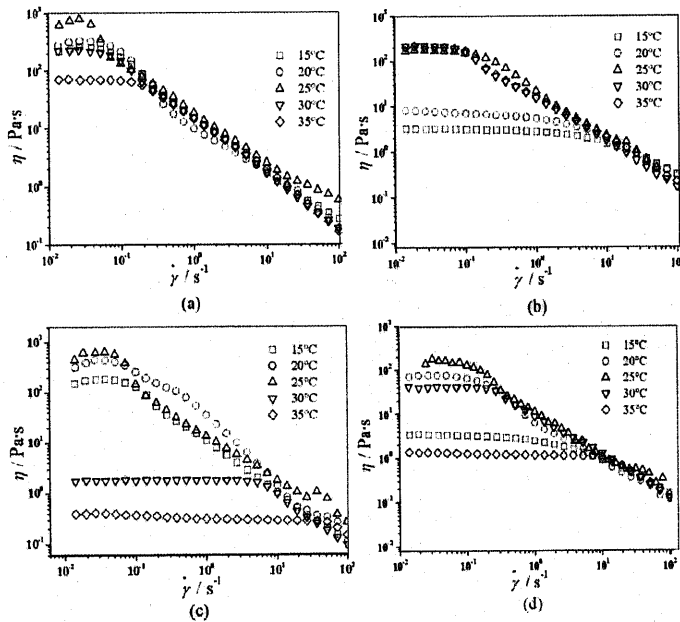
Figure 4.1. Effect of Temperature on the steady-shear rheology of 0.06 M (excluding cosurfactant) $ChEO_m$ (m = 15, 30) containing different mixing fraction (X) of $C_{12}EO_3$:

(a) $ChEO_{30}$-$C_{12}EO_3$, X = 0.77, (b) $ChEO_{30}$-$C_{12}EO_3$, X = 0.74, (c) $ChEO_{15}$-$C_{12}EO_3$, X = 0.62, (d) $ChEO_{15}$-$C_{12}EO_3$, X = 0.6.
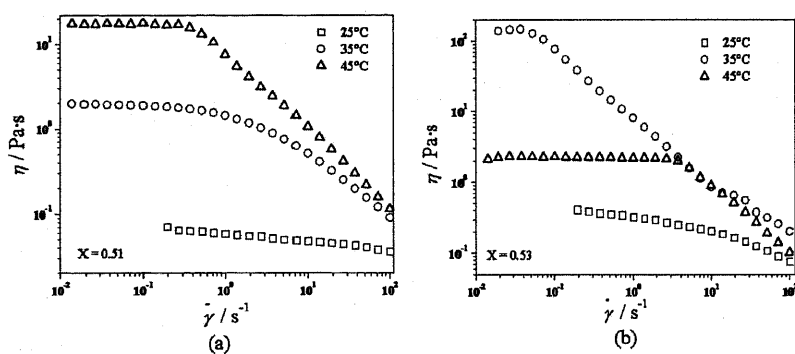
Figure 4.2. Effect of Temperature on the steady-shear rheology of 0.06 M (excluding cosurfactant) $ChEO_{15}$ containing different mixing fraction (X) of monolaurin: (a) $X = 0.51$; (b) $X = 0.53$.

point is below 40 °C and so there are no data. For clarity of presentation we present the data of only the most viscous systems at various temperatures (Figures. 4.1, 4.2).

The aqueous 0.06 M $ChEO_{30}$ solution containing $C_{12}EO_3$ ($X = 0.77$) is remarkable in that the plots at different temperatures almost superimpose at all shear-rates (Figure 4.1a). However, at high shear-rates nonlinear effects and shear-induced structure formation complicates the understanding and so we discuss mainly the low-shear data below. The low-shear viscosity values of the aqueous 0.06 M $ChEO_{30}$ solution containing $C_{12}EO_3$ ($X = 0.77$) system (Figure 4.1a) and the aqueous 0.06 M $ChEO_{30}$ solution containing $C_{12}EO_3$ ($X = 0.74$) system (Figure 4.1b) manifest lower order of magnitude variation than those of the aqueous 0.06 M $ChEO_{15}$ solution containing $C_{12}EO_3$ ($X = 0.62$) system (Figure 4.1c) and the aqueous 0.06 M $ChEO_{15}$ solution containing $C_{12}EO_3$ ($X = 0.6$) system (Figure 4.1d). We point out that the difference between the first pair and the second is that $ChEO_{30}$ used in the first pair has a larger head-group than that of $ChEO_{15}$ in the latter. Also, the systems in Figures 4.1 a and c reaches very high ($\sim 10^3$ Pa·s) low-shear viscosities at 25 °C. For the systems in Figures 4.1 b and d only $\sim 10^2$ Pa·s viscosity is achieved and the variation

53

of low-shear viscosity is greater at low temperatures and lower at high temperatures whereas the opposite is observed for the systems in Figures 4.1 a and c. We notice that, for all systems in Figure 4.1, at all temperatures, shear-thinning is observed, that is above a critical shear-rate $\dot{\gamma}_c$, the viscosity falls rapidly with increasing shear. This non-Newtonian behavior is an indication of formation of network structures of long wormlike micelles, which is also supported by the observation of shear birefringence in the samples. Shear-thinning occurs due to alignment of aggregates under flow if the deformation is faster than the time required to regain an equilibrium network structure, and with increasing network density the relaxation becomes slower; i.e., shear thinning begins at a lower shear rate. The zero-shear viscosity (η_0), an important rheological quantity, has been obtained by extrapolating the low shear plateau data. In the cases where the low shear-rate viscosity is high, beginning of shear-thinning is observed at lower shear-rates, which indicates increased structuring in the material. In Figure 4.1 and Figure 4.2b we notice that the low-shear viscosity first increases, reaches a maximum and then decreases as temperature is increased. Lower viscosity usually implies shorter average micellar contour length. But in our case, we argue that the decrease in viscosity at high temperature is due to micellar junction formation, supported by dynamic rheological data presented below. These junctions are labile and unlike physical cross-links in polymer gels, promote faster stress relaxation. Such branched micellar networks should also behave as non-Newtonian fluids and so shear-thinning is observed at high shear-rates (Figures 4.1, 4.2b). The system in Figure 4.2a manifests simple rise in low-shear viscosity and decrease in critical shear-rate with increasing temperature, suggesting mainly micellar growth with temperature rise in the temperature range of investigation. Also, this system is Newtonian at low temperature.

The systems in Figures 4.1 and 4.2 are all formed at rather high cosurfactant composition. For low cosurfactant compositions (data not presented) we did not observe any shear-thinning or shear birefringence. The significance of these results is discussed further below.

4.3.2 Dynamic rheology

To study the viscoelastic properties of the wormlike micellar solutions in the above systems, oscillatory shear measurements have been performed. Figure 4.3 shows the variation of the elastic or storage modulus (G') and the viscous or loss modulus (G'') with oscillation frequency at different temperatures for the aqueous 0.06 M $ChEO_m$ solutions containing $C_{12}EO_3$ with those $C_{12}EO_3$ concentrations that form highly viscous solutions. In the aqueous 0.06 M $ChEO_{15}$ solutions containing monolaurin, viscoelasticity is indicated in dynamic measurements only at high temperatures for the most viscous compositions. Such small quantity of data is not much useful for comparison and so we do not graphically present them here. In the aqueous 0.06 M $ChEO_{30}$ solutions containing monolaurin, all compositions are fluid at all temperatures. Therefore, we did not perform dynamic rheometry for this system.

In the systems of Figure 4.3, liquid-like behavior ($G' < G''$) is observed in the low-frequency region, but both G' and G'' increase with ω and viscoelastic behavior ($G' > G''$) is observed in the high-frequency region. The cross-over occurs at the longest relaxation time, the terminal relaxation time τ_R, of the system.

The η_0 values for the Newtonian systems of low viscosity have been obtained by extrapolating the viscosity to zero-shear rate. For viscoelastic systems
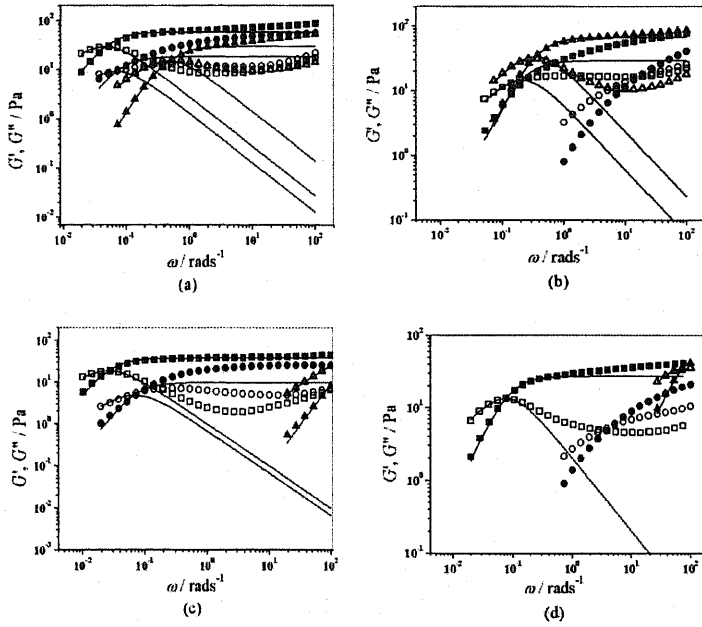
Figure 4.3. Effect of Temperature on the dynamic rheology of 0.06 M (excluding

cosurfactant) $ChEO_m$ (m = 15, 30) containing different mixing fraction (X) of $C_{12}EO_3$

: (a) $ChEO_{30}$-$C_{12}EO_3$, X = 0.77, (b) $ChEO_{30}$-$C_{12}EO_3$, X = 0.74, (c) $ChEO_{15}$-$C_{12}EO_3$, X

= 0.62, (d) $ChEO_{15}$-$C_{12}EO_3$, X = 0.6. Legends: filled symbols G', open symbols G'' -

15 °C ●○; 25 °C ■□; 35 °C ▲△. The lines are the best fit to the Maxwell model.

following Maxwellian behavior at low-shear frequency, η_0 values were estimated from

the following relation involving the plateau modulus (G_0) and the terminal relaxation

time (τ_R):

$$\eta_0 = G_0 \tau_R \tag{4-1}$$

Alternately, the following relationship allows one to estimate η_0 by extrapolating the

complex viscosity values ($| \eta^* |$) to zero shear frequency:

$$|\eta^*| = \frac{\left(G'^2 + G''^2\right)^{1/2}}{\omega} = \frac{\eta_0}{\sqrt{1 + \omega^2 \tau_R^2}} \tag{4-2}$$

The values of viscoelastic samples obtained from the estimated values of G_0 and τ_R are only approximate values.

The viscoelastic behavior of the entangled micelles is described by the Cates model,[23 - 25] which considers two processes of stress relaxation – reptation or the reptile-like motion of the micelle along a tube and the reversible scission of micelles – taking place on two time scales, namely, the reptation time τ_{rep} and the breaking time τ_b. The viscoelastic behavior of such a system at low shear frequency often follows the Maxwell model of viscoelastic fluids with a single relaxation time τ_R given by $(\tau_b.\tau_{rep})^{1/2}$ and plateau modulus (G_0) described by Equations. 4-3 and 4-4[31]:

$$G'(\omega) = \frac{\omega^2 \tau_R^2}{1 + \omega^2 \tau_R^2} G_0 \tag{4-3}$$

$$G''(\omega) = \frac{\omega \tau_R}{1 + \omega^2 \tau_R^2} G_0 \tag{4-4}$$

The Maxwell material is characterized by a clear maximum in the G'' curve, a plateau in the G' curve at high frequency, and a cross-over of the two curves at the G'' maximum. The τ_R obtained from experiment is well approximated by the relaxation time appearing in the model. In cases where the maximum in G'' and the plateau in G' are not clear, we did not try to fit to Maxwell model (data for 15 °C in Figure 4.3 b and d). The systems in Figure 4.3b and d are the aqueous 0.06 M $ChEO_{30}$ solution containing $C_{12}EO_3$ ($X = 0.74$) and the aqueous 0.06 M $ChEO_{15}$ solution containing $C_{12}EO_3$ ($X = 0.6$), respectively. Since the cosurfactant content is comparatively lower in these systems than the aqueous 0.06 M $ChEO_{30}$ solution containing $C_{12}EO_3$ ($X = 0.77$) in Figure 4.3a and the aqueous 0.06 M $ChEO_{15}$ solution containing $C_{12}EO_3$ ($X = 0.62$) in Figure 4.3c, at low temperatures the average interfacial curvature is expected

to be high for the systems in Figure 4.3 b and d, and so, shorter micelles should abound, giving low relaxation times (0.07s in the former and 0.44s in the latter) and stronger deviation from the Maxwell model. Such deviations are not observed for the systems in Figure 4.3 a and c, which in fact have rather low cross-over frequency at low temperatures, indicating higher relaxation time on account of the rather slow reptation of large micelles. This high relaxation time correlates well with the high low-shear viscosity of the same systems (Figure 4.1a and c). Also, at high frequencies, in each system in Figure 4.3, the G' and the G'' plots make positive deviation from the prediction of Maxwell model. This type of upturn is usually attributed to stress relaxation by local motions or small length-scale motions in the system. Due to this upturn at high frequencies, it is not easy to get an idea of the elasticity of the systems directly from the data. Fitting to the Maxwell data gives an estimate of the lower bound of the possible plateau modulus values. In the data presented in Figure 4.3 we notice that for each system, the cross-over frequency shifts from high to low value and again rises as temperature is gradually increased. This corresponds well with the shift of steady-rate zero-shear viscosity with temperature for the same systems (Figure 4.1). This suggests some structural change with temperature rise, which allows faster stress relaxation in the high temperature domain. Consideration of both the relaxation times and the plateau modulus indicates that this change is due to increased micellar branching. Also, the variation of the cross-over frequency with temperature for the aqueous 0.06 M $ChEO_{30}$ solution containing $C_{12}EO_3$ ($X = 0.77$) in Figure 4.3a and for the aqueous 0.06 M $ChEO_{30}$ solution containing $C_{12}EO_3$ ($X = 0.74$) in Figure 4.3b is order of magnitude lower than that for the aqueous 0.06 M $ChEO_{15}$ solution containing $C_{12}EO_3$ ($X = 0.62$) in Figure 4.3c and the aqueous 0.06 M $ChEO_{15}$ solution containing $C_{12}EO_3$ ($X = 0.6$) in Figure 4.3d. Again, this corresponds well with the variation of the

steady low-shear viscosity with temperature of these systems shown in Figure 4.1 and can be attributed to the difference in the head-group sizes of $ChEO_{15}$ and $ChEO_{30}$. Discussions of these results are presented below.

4.4 Discussion

4.4.1 Effect of hydrophilic surfactant head-group size

Figure 4.4. Variation of zero-shear viscosity with temperature and cosurfactant mixing fraction (X) for the 0.06 M (excluding cosurfactant) $ChEO_m$ systems: (a) $ChEO_{15}$-$C_{12}EO_3$, (b) $ChEO_{30}$-$C_{12}EO_3$, (c) $ChEO_{15}$-monolaurin, (d) $ChEO_{30}$-monolaurin. Lines are meant to be guide for the eye only.

In Figure 4.4 we present the summary of the zero-shear viscosity data of the several systems at different temperatures. The order of magnitude rise in the viscosity at certain X value (cosurfactant composition) is indication of the formation of long micelles, supported by shear-thinning, flow birefringence and isotropy at rest, which are characteristics not shared by surfactant liquid crystals and sponge phase. The value of X at which viscosity dramatically rises, if such rise is present, shifts to lower value upon increase in the temperature (Figure 4.4). It is evident from Figure 4.4 that the viscosity in the 0.06 M aqueous $ChEO_{30}$ systems is much less sensitive to temperature variation than that in the 0.06 M aqueous $ChEO_{15}$ systems. In the 0.06 M aqueous $ChEO_{30}$ solutions containing monolaurin there is no indication of long micelle formation at any temperature. In fact the plots of the system are approximately flat and almost superimposed (Figure 4.4d). However, this fact, coupled with the result that the viscosity rises in the 0.06 M aqueous $ChEO_{15}$ solution containing monolaurin at certain X value and the shift of this value with temperature (Figure 4.4c) is indirect

support of the fact that the $ChEO_{30}$ systems are less temperature sensitive than the $ChEO_{15}$ systems. Thus, increase of the POE chain length of surfactant can reduce the temperature sensitivity of the viscosity of wormlike micellar solutions.
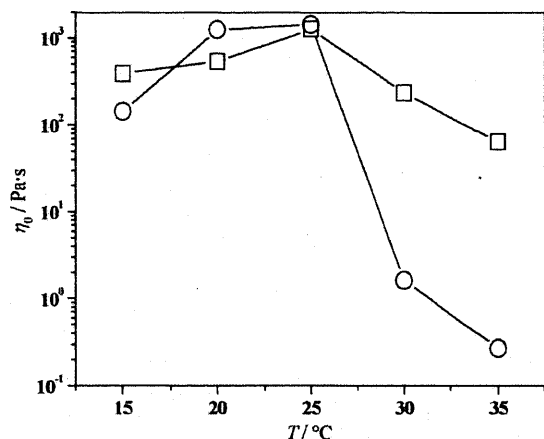

Figure 4.5. Variation of the zero-shear viscosity of the most viscous aqueous 0.06 M $ChEO_{15}$ solution containing $C_{12}EO_3$ ($X = 0.62$) (O) and the most viscous aqueous 0.06 M $ChEO_{30}$ solution containing $C_{12}EO_3$ ($X = 0.77$) ($\square$) with temperature. Lines are meant to be guide for the eye only.

Figure 4.6. Variation of the relaxation time (a) and plateau modulus (b) of the most viscous aqueous 0.06 M $ChEO_{15}$ solution containing $C_{12}EO_3$ ($X = 0.62$) (O) the most viscous aqueous 0.06 M $ChEO_{30}$ solution containing $C_{12}EO_3$ ($X = 0.77$) ($\square$) with temperature. Lines are meant to be guide for the eye only.
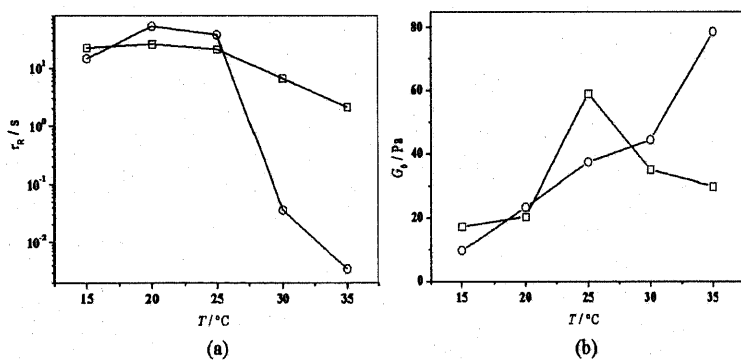
To bring the point in focus, we separately present the zero-shear viscosity data of the aqueous 0.06 M $ChEO_{15}$ solution containing $C_{12}EO_3$ ($X = 0.62$) and the

aqueous 0.06 M $ChEO_{30}$ solution containing $C_{12}EO_3$ ($X = 0.77$) in Figure 4.5. These are the most highly viscous solutions, with the same order of magnitude zero-shear viscosity ($\sim 10^3$ Pa·s) at 25°C, found in the two systems. The cosurfactant mole fractions are different, but since highly viscous solutions are formed in either systems in such a small composition regime that this mismatch is unavoidable. Both plots rise and following a maximum, fall as temperature is increased. Clearly, for the first system, in the temperature range studied, the maximum viscosity obtained is more than 3 orders of magnitude higher than the minimum viscosity obtained. In the latter system the difference is less than 2 orders of magnitude. We also present the terminal relaxation time of the same systems in Figure 4.6a. The order of magnitude differences in the variation of the relaxation times of the two systems are similar to those for the zero-shear data (Figure 4.6a).

Referring to Figure 4.5, it should be mentioned that a truly temperature-insensitive system would yield a horizontal viscosity-temperature plot. The aqueous 0.06 M $ChEO_{30}$ solution containing $C_{12}EO_3$ ($X = 0.77$) comes closer to reaching this ideal, compared to the aqueous 0.06 M $ChEO_{15}$ solution containing $C_{12}EO_3$ ($X = 0.62$). In case of the commonly studied ionic wormlike systems, only monotonic decrease of viscosity with increasing temperature has been observed.[5, 21] In ionic systems, the translational entropy contribution of the micellar end-caps favors shorter micelles with greater net end-cap density and overcomes the end-cap energy as the temperature is raised. In POE surfactants the effect of temperature on the surfactant spontaneous curvature is dominant over the usual entropy/energy balance.[32] From our results in Figure 4.5 we notice that temperature sensitivity of the micellar growth, which is determined by the interfacial curvature, can be tuned by changing the POE chain

length. Thus the importance of using very long chain POE surfactant like $ChEO_{30}$ to form wormlike micelle is clear. We discuss this point further below.

At lower temperatures, the viscosity rises with temperature in the systems in Figure 4.5. There is a corresponding rise in the relaxation times as seen in Figure 4.6a. Since relaxation time is an indication of linear micellar growth, the viscosity increase in the low temperature range can be attributed to mainly the increase in average micelle contour length due to curvature reduction with temperature. As we have mentioned in the introduction, for POE surfactant wormlike micelles, the drop that follows the rise of the zero-shear viscosity with temperature rise, as observed in our data is explained by the predominance of the formation of three-fold junctions with rise in temperature. These junctions have lower local curvature, and are favored by higher temperature in POE surfactants. These junctions are quite fluid, and can slide along the micellar contour. This motion provides a very fast stress relaxation mechanism. Thus although the branched micelles formed by such junctions have higher network density, the relaxation time is quite low. Therefore, the viscosity of branched micellar network is also low. Cates' model has been extended to branched micelles, and it has been demonstrated that all the results concerning the rheology of linear micelles can be applied to branched micelles, if instead of the average micellar contour length L by L_c is used throughout, where L_c represents the harmonic mean between the average distance from one point along the micelle to the first cross-link and the average distance from that point to the first end-cap, or equivalently, the ratio of the total length over the concentration of end-caps plus twice that of junctions.[33] In this definition, we notice that the junction density contributes more toward reducing L_c than the end-cap density. Now from Figure 4.6a we see that the relaxation times go through a maximum as temperature is raised both for the aqueous 0.06 M $ChEO_{15}$

solution containing $C_{12}EO_3$ ($X = 0.62$) and for the aqueous 0.06 M $ChEO_{30}$ solution containing $C_{12}EO_3$ ($X = 0.77$), although for the latter the maximum, occurring at 20 °C, is not strongly peaked. This reflects that L_c, as defined above, passes through a maximum value in either system. The relaxation times at 15 °C in the aqueous 0.06 M $ChEO_{15}$ solution containing $C_{12}EO_3$ at $X = 0.62$ (~15 s) is smaller than that in the aqueous 0.06 M $ChEO_{30}$ solution containing $C_{12}EO_3$ at $X = 0.77$ (~23 s). Therefore, at this temperature, we may assume slightly higher end-cap density in the former system compared to the latter which is justified by the smaller net content of the hydrophobic $C_{12}EO_3$ in the former system compared to the latter. If the ratio of the hydrophilic surfactant, which in this case is $ChEO_m$, compared to the hydrophobic cosurfactant is large, the hydrophilic molecules can be accommodated in the high curvature end-caps by increasing their density.[32] As temperature is raised, the end-cap density decreases and produces a rise in the relaxation time. Thus, at the low temperature zone, the relaxation time of the aqueous 0.06 M $ChEO_{15}$ solution containing $C_{12}EO_3$ at $X = 0.62$ increases faster than that of the aqueous 0.06 M $ChEO_{30}$ solution containing $C_{12}EO_3$ at $X = 0.77$, reflecting again the greater temperature sensitivity of the interfacial curvature of shorter POE chain surfactants (Figure 4.6a). However, at intermediate temperatures, junction formation becomes predominant and the relaxation time drops. The sharper fall of the relaxation time following the maximum in the aqueous 0.06 M $ChEO_{15}$ solution containing $C_{12}EO_3$ ($X = 0.62$) as compared to the aqueous 0.06 M $ChEO_{30}$ solution containing $C_{12}EO_3$ ($X = 0.77$) indicates that in the former system stronger temperature induced curvature reduction favors greater formation of low local-curvature junctions in the high temperature regime, which reduces L_c more strongly, compared to the latter system (Figure 4.6a). Of course, formation of shorter micelles with greater end-cap density and lower entanglement density would reduce

the relaxation time, but would also reduce the elastic modulus. Increase in the junction density of entangled network can increase the elasticity of the system. We have found, as shown in Figure 4.6b, the modulus increases with temperature for the aqueous 0.06 M $ChEO_{15}$ solution containing $C_{12}EO_3$ (X = 0.62), but for the aqueous 0.06 M $ChEO_{30}$ solution containing $C_{12}EO_3$ (X = 0.77) system it passes through a maximum and then does not change appreciably as temperature is raised. This kind of decrease in the elastic modulus with decrease in micellar interfacial curvature has been observed in other systems.[34 - 35] The explanation invoked is the formation of saturated, multi-connected network without any entanglement, whose elasticity would be lower than the elasticity of a network containing both entanglements and junctions. The fact that the modulus does not change appreciably after a sharp fall, as can be seen in Figure 4.6b, provides confidence in assuming that in the aqueous 0.06 M $ChEO_{30}$ solution containing $C_{12}EO_3$ (X = 0.77), saturated network forms at high temperature. Thus, from considerations of the dynamic rheology results in Figure 4.6, the fall in viscosity of the same systems (Figure 4.5) with temperature rise can be ascribed to increase in micellar junction density due to curvature reduction. The alternative assumption of increasing end-cap density due to the formation of shorter micelles can be rejected because end-caps are not favored by reduced curvature and decrease in micelle contour length cannot increase the elastic modulus.

We ascribe the origin of the difference between the aqueous 0.06 M $ChEO_{15}$ solution containing $C_{12}EO_3$ (X = 0.62) and the aqueous 0.06 M $ChEO_{30}$ solution containing $C_{12}EO_3$ (X = 0.77) systems mainly to the difference in the size of the POE chains. NMR investigation of dodecyl oligoethylene oxide surfactant solutions indicate that the water of hydration of POE chains decreases mainly from the innermost ethylene oxide groups at increasing temperatures.[28] This implies less

reduction of the curvature, and therefore less micellar growth, for the surfactant of longer POE chain upon increasing temperature, since at any temperature a longer chain will retain more water than a shorter chain. This is experimentally verified by recent investigations on alkyl POE surfactants, in agreement with molecular thermodynamic models.[27, 36] Thus, we can assume that with temperature rise the dehydration of POE chains of $ChEO_{15}$ causes greater curvature reduction compared to $ChEO_{30}$.

We focused on the difference between the aqueous 0.06 M $ChEO_{15}$ solution containing $C_{12}EO_3$ and the aqueous 0.06 M $ChEO_{30}$ solution containing $C_{12}EO_3$ systems for different X values. Of course, at $X = 0.77$, the aqueous 0.06 M $ChEO_{15}$ solution containing $C_{12}EO_3$ is phase separated and therefore comparison cannot be made. The viscosity of the aqueous 0.06 M $ChEO_{30}$ solution containing $C_{12}EO_3$ at $X = 0.62$ is not very high at any temperature, indicating poor micellar growth (Figure 4.4b). Therefore, appropriate comparison cannot be made with the aqueous 0.06 M $ChEO_{15}$ solution containing $C_{12}EO_3$ at $X = 0.62$. So, we chose the most viscous systems for detailed comparison.

4.4.2 Effect of the cosurfactant fraction and type

In Figure 4.7 we present the viscosity-temperature plot of the aqueous 0.06 M $ChEO_m$ solution containing $C_{12}EO_3$ for X values that form highly viscous solutions. The maxima in the viscosity-temperature plot is a general feature in these systems, implying predominantly growth in micellar contour length followed by mainly branching and later perhaps saturation by branch points, all due to average curvature reduction with increasing temperature. Before the maximum is reached contour length increase is the main contribution, whereas following the maximum, increased

branching is the dominant process. In Figure 4.7a, we notice that for the lower $C_{12}EO_3$

concentration ($X = 0.6$) viscosity rise in the low temperature region is sharper (the

slope of the low temperature branch of the plot is steeper) and viscosity fall in the high

temperature region is weaker (the high temperature branch, following the maximum of

the plot, is less steep) than those for the higher cosurfactant composition ($X = 0.62$).

This behavior is seen with the aqueous 0.06 M $ChEO_{30}$ solution containing $C_{12}EO_3$
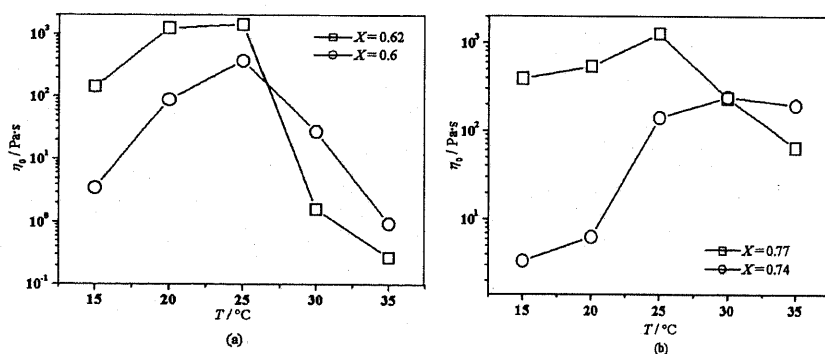

Figure 4.7. Comparison of the variation of the zero-shear viscosity with temperature

0.06 M (excluding cosurfactant) solution of $ChEO_m$ for different mixing fraction (X)

of cosurfactant: (a) $ChEO_{15}$-$C_{12}EO_3$, (b) $ChEO_{30}$-$C_{12}EO_3$.
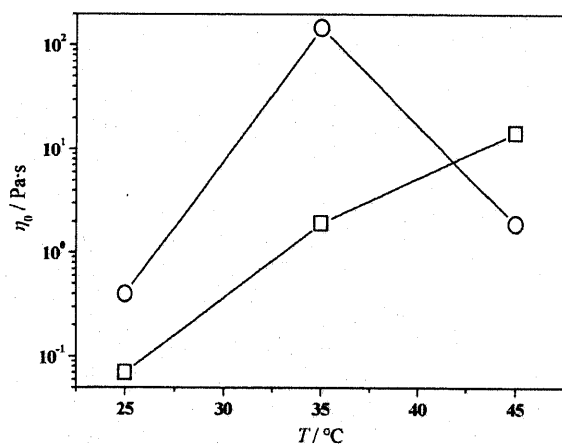

Figure 4.8. Variation of zero-shear viscosity of 0.06 M (excluding cosurfactant)

$ChEO_{15}$ solution containing monolaurin systems for different mixing fractions (X)
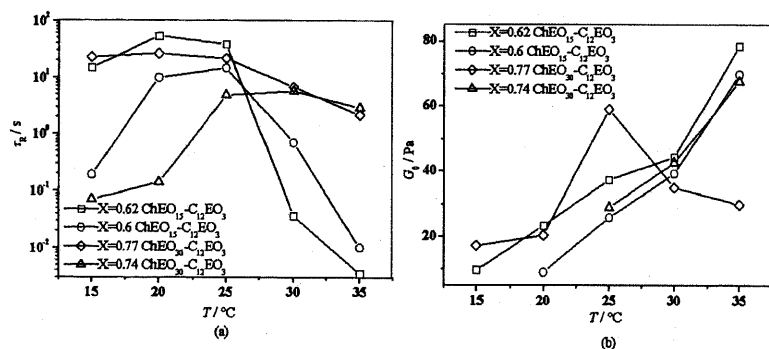
with temperature.

Figure 4.9. Variation of the terminal relaxation times and the plateau modulus of 0.06 M (excluding cosurfactant) $ChEO_m$ (m = 15, 30) solution for different mixing fractions (X): (a) relaxation time, (b) plateau modulus.

also (Figure 4.7b). It appears that for the higher cosurfactant compositions in either system, the average interfacial curvature is sufficiently reduced at any temperature so that there is always some tendency of formation of low local-curvature junction points. Such coexistence of junctions and end-caps, that is branched and cylindrical micelles has been observed by cryo-TEM in nonionic surfactant systems even at 18 °C.[37] Increase in temperature reduces the average interfacial curvature of the micellar interface and therefore allows for both elongation of the cylindrical body of the micelles (which has lower curvature than that of end-caps) as well as increase in the density of the low local-curvature junction points.[38] In other words, temperature rise favors both micellar growth and branching, although branching becomes significant for the lower cosurfactant compositions (higher average curvature) only at rather high temperatures (Figure 4.7). Whereas micellar growth favors increase in viscosity, branching lowers the viscosity due to the faster relaxation process of the sliding movement of the fluid junctions. Thus, with temperature rise, the increase in the junction density of the lower average curvature systems in Figure 4.7 compensates

somewhat for the micellar growth induced viscosity rise in the lower temperature zone and results in rather flat viscosity-temperature plots. Since at higher temperature, lower average curvature allows for more low local-curvature junctions, following the temperature at which branching becomes predominant, junction density increases more rapidly for the same high cosurfactant content systems in Figure 4.7 and the viscosity falls much more sharply due to the faster relaxation processes of the sliding movement of junctions. The relaxation times in Figure 4.9a can be seen to behave in manner quite similar to the viscosity of the same systems in Figure 4.7. This is understandable, since the relaxation time reflects the magnitude of L_c, a quantity which is decreased due to increase in both end-cap density and junction density of a system.[33] Thus, we can explain the slow rise in the relaxation times in the aqueous 0.06 M $ChEO_{30}$ solution containing $C_{12}EO_3$ system ($X = 0.77$) and the aqueous 0.06 M $ChEO_{15}$ solution containing $C_{12}EO_3$ system ($X = 0.62$) at low temperatures due to decrease in end-cap density and increase in junction density, two effects which oppose each other toward increasing L_c. At high temperature, junction formation becomes predominant and L_c falls, thereby reducing the relaxation time. In the aqueous 0.06 M $ChEO_{30}$ solution containing $C_{12}EO_3$ ($X = 0.74$) and aqueous 0.06 M $ChEO_{15}$ solution containing $C_{12}EO_3$ ($X = 0.6$) systems, which have higher average interfacial curvature due to lower cosurfactant ratios, low local-curvature junction formation is less probable than in the low average interfacial curvature aqueous 0.06 M $ChEO_{30}$ solution containing $C_{12}EO_3$ ($X = 0.77$) and the aqueous 0.06 M $ChEO_{15}$ solution containing $C_{12}EO_3$ ($X = 0.62$), respectively. In fact the relaxation times at 15 °C for the aqueous 0.06 M $ChEO_{15}$ solution containing $C_{12}EO_3$ at $X = 0.6$ (~ 0.44 s) and the aqueous 0.06 M $ChEO_{30}$ solution containing $C_{12}EO_3$ at $X = 0.74$ (~ 0.07 s) is much lower than respectively the aqueous 0.06 M $ChEO_{15}$ solution containing $C_{12}EO_3$

68

at $X = 0.62$ (~ 15 s) and the aqueous 0.06 M $ChEO_{30}$ solution containing $C_{12}EO_3$ at X = 0.77 (~ 23 s), indicating much larger end-cap density in the first two systems (Figure 4.9a). Temperature rise reduces the average interfacial curvature and the end-cap density decreases, giving sharp rise in the relaxation time. Thus, L_c and therefore relaxation time rise faster in the low temperature region and falls slower in the high temperature zone in the aqueous 0.06 M $ChEO_{30}$ solution containing $C_{12}EO_3$ (X = 0.74) and in the aqueous 0.06 M $ChEO_{15}$ solution containing $C_{12}EO_3$ ($X = 0.6$) than in the aqueous 0.06 M $ChEO_{30}$ solution containing $C_{12}EO_3$ ($X = 0.77$) and in the aqueous 0.06 M $ChEO_{15}$ solution containing $C_{12}EO_3$ ($X = 0.62$), respectively (Figure 4.9a). The plateau modulus presented in Figure 4.9b reflects the entanglement density of the measured system, which depends on the net surfactant volume fraction. Since the total surfactant content in our systems are differs from one to another, we do not make any direct comparison. However, we point out the fact that except for the aqueous 0.06 M $ChEO_{30}$ solution containing $C_{12}EO_3$ ($X = 0.77$), all the systems in Figure 4.9b manifest an increase in the modulus with temperature rise, even in the temperature zone where relaxation times fall for the same systems (Figure 4.9a). This can be only explained by the increase in the low local-curvature junction points due to decrease in the average interfacial curvature with increasing temperature. Also as discussed in the previous section, the sharp fall in the modulus at high temperature in the aqueous 0.06 M $ChEO_{30}$ solution containing $C_{12}EO_3$ ($X = 0.77$) can be explained as the formation of saturated network having low elasticity, again due to the decrease in average interfacial curvature. Thus, the sole concept of the reduction of the average interfacial curvature with temperature can consistently explain all the observations and the dynamic rheological data supports and complements the steady shear-rate data nicely

as well as providing valuable insights into the structural changes induced by temperature.

In the 0.06 M aqueous $ChEO_{15}$ solution containing monolaurin (Figure 4.8), the trend seems to be different. In fact, for $X = 0.53$ the viscosity passes through a high value ($\sim 10^2$ Pa·s) maximum followed by a drop upon increasing temperature. Dynamic measurements, for which we did not present data, reveals that the drop in zero-shear viscosity corresponds with drop in relaxation time and increasing plateau modulus, implying predominant micellar branching with increasing temperature. For $X = 0.51$, the monotonous but slow rise of viscosity with temperature corresponds with similar monotonous rise in relaxation time and modulus, implying linear micellar growth dominating over branching. The data obtained starts from 25 °C. At this temperature the maximum viscosity achieved is not very high, implying low micellar growth and greater average interfacial curvature. Thus, there is expected to be little tendency for low local-curvature junction formation at low temperatures. Since monolaurin does not have POE head-group, $ChEO_{15}$ is the only component expected to contribute to temperature induced curvature reduction in this system. Since the POE chain of $ChEO_{15}$ is quite large, if its fraction is higher in the solution, the amount of water of hydration will also be higher. Therefore, with increasing temperature, the net water of hydration removed from the POE layer will be less for that solution which contains the larger ratio of $ChEO_{15}$. Thus, the reduction of average interfacial curvature upon increasing temperature should be less for the higher $ChEO_{15}$ fraction, i.e. the lower monolaurin fraction system. This would imply higher temperature sensitivity for the higher monolaurin composition system, which is actually observed (Figure 4.8).

As mentioned above, in the 0.06 M aqueous $ChEO_{30}$ solutions containing monolaurin, micellar growth is not observed at any temperature. So, we cannot effectively compare this system with the aqueous 0.06 M $ChEO_{30}$ solutions containing $C_{12}EO_3$.

4.5. Conclusion

We report the first indication of the possibility of making wormlike micelle solution possessing low sensitivity toward temperature-induced changes in rheological properties. We have found that for wormlike micelles formed from long POE chain cholesteryl ether surfactants with addition of appropriate cosurfactants, the temperature sensitivity of the viscosity and relaxation time of the solutions can be reduced if the POE chain length is increased. Due to dehydration of the POE chains with increasing temperature, the curvature of the micellar interface decreases and micelles become progressively longer and ultimately branched through junction formation. As a result, the viscosity passes through a maximum at some temperature. The extent of the variation of viscosity in different temperature zones may also be changed by changing the cosurfactant content. Subtle changes can occur due to changes in cosurfactant mixing ratio and type. Since the changes of the rheological properties with temperature can be explained by the transformation of micelles from cylindrical to branched, which is ultimately determined by a sensitive interplay of end-cap and junction densities, our results intimate the potential of more fruitful research toward fine-tuning these quantities.

The implication of temperature-insensitive wormlike micelles for the industry is clear. We can name shampoos, detergents etc. as a few examples. On the scientific side, the development of temperature-insensitive wormlike micellar solutions would

71

require changes in the theoretical approach to such systems. Since rheological data can be easily obtained and temperature is an important thermodynamic parameter that can be efficiently tuned without making internal changes in a system, any theoretical derivation can be quickly tested. A well-developed analogy between the solution behavior of POE surfactant micelles and microemulsion and that of dipolar fluids composed of magnetic colloidal nano-particles imply that such progress can benefit the whole of colloid science in general.[39]

References

[1]☐ P. Debye, E. W. Anacker, J. Phys. Colloid Chem. 55 (1951) 644

[2]☐ N. Pilpel, J. Phys. Chem. 60 (1956) 779

[3]☐ G. Porte, J. Phys. Chem. 87 (1983) 3541

[4]☐ C. A. Dreiss, Soft Matter 3 (2007) 956-970.

[5]☐ L. J. Magid, J. Phys. Chem. B 102 (1998) 4064-4074.

[6]☐ H. Kunieda, C. Rodriguez, Y. Tanaka, M. H. Kabir, M. Ishitobi, Colloids Surf. B 38 (2004) 127-130.

[7]☐ C. Rodriguez, D. P. Acharya, K. Hattori, T. Sakai, H. Kunieda, Langmuir 19 (2003) 8692-8696.

[8]☐ K. Trickett, J. Eastoe, Adv. Colloid Interface Sci. 144 (2008) 66–74

[9]☐ D. P. Acharya, K. Hattori, T. Sakai, H. Kunieda, Langmuir 19 (2003) 9173-9178.

[10]☐ D. P. Acharya , D. Varade , K. Aramaki , J. Colloid and Interface Science 315 (2007) 330–336

[11]☐ D. Varade, K. Ushiyama, L. K. Shrestha, K. Aramaki, J. Colloid Interface Sci. 312 (2007) 489-497.

[12] C. Rodriguez, D. P. Acharya, A. Maestro, K. Hattori, H. Kunieda, J. Chem. Eng. Soc. Jpn. 37 (2004) 622-629.

[13] D. P. Acharya, M. K. Hossain, J. Feng, T. Sakai, H. Kunieda, Phys. Chem. Chem. Phys. 6 (2004) 1627-1631.

[14] A. Maestro, D. P. Acharya, H. Furukawa, J. M. Gutierrez, M. A. Lopez-Quintela, M. Ishitobi, H. Kunieda, J. Phys. Chem. B 108 (2004) 14009-14016.

[15] H. Rehage, H. Hoffmann, J. Phys. Chem. 92 (1988) 4712-4719.

[16] D. P. Acharya, S. C. Sharma, C. Rodriguez-Abreu, and K. Aramaki, J. Phys. Chem. B 110 (2006) 20224-20234.

[17] D. P. Acharya, H. Kunieda, J. Phys. Chem. B 107 (2003) 10168-10175.

[18] C. Rodriguez, K. Aramaki, Y. Tanaka, M. A. Lopez-Quintela, M. Ishitobi, H. Kunieda, J. Colloid Interface Sci. 291 (2005) 560-569.

[19] T. Sato, D. P. Acharya, M. Kaneko, K. Aramaki, Y. Singh, M. Ishitobi, H. Kunieda, J. Disp. Sci. Technol. 27 (2006) 611-616.

[20] S. Candau, E. Hirsch, R. Zana, J. Colloid Interface Sci. 105 (1985) 521.

[21] M. E. Cates, S. J. Candau, J. Phys. Condens. Matter 2 (1992) 6869-6892.

[22] T. J. Drye, M. E. Cates, J. Chem. Phys. 96 (1992) 1367-1375.

[23] M. E. Cates, Macromolecules 20 (1987) 2289-2296.

[24] R. Granek, M. E. Cates, J. Chem. Phys. 96 (1992) 4758-4767.

[25] M. E. Cates, J. Phys. France 49(1988) 1593-1600.

[26] T. Sato, M. K. Hossain, D. P. Acharya, O. Glatter, A. Chiba, H. Kunieda, J. Phys. Chem. B 108 (2004) 12927.

[27] O. Glatter, G. Fritz, H. Lindner, J. Brunner-Popela, R. Mittelbach, R. Strey, Langmuir 16 (2000) 8692.

[28] M. Jonstromer, B. Jonsson, B. Lindman, J. Phys. Chem. 95 (1991) 3293-3300.

[29] D. Varade, C. Rodriguez, L. K. Shrestha, K. Aramaki, J. Phys. Chem. B 111 (2007) 10438-10447.

[30] T. Ahmed, K. Aramaki, J. Colloid Interface Sci. 327 (2008) 180-185.

[31] R. G. Larson, The Structure and Rheology of Complex Fluids; Oxford University Press: New York, 1999; Chapter 12.

[32] N. Dan, S. A. Safran, Adv. Colloid Interface Sci. 123-126 (2006) 323-331.

[33] F. Lequeux, Europhys. Lett. 19 (1992) 675.

[34] S. J. Candau, A. Khatory, F. Lequeux, F. Kern, J. de Phys. IV 3 (1993) 197-209.

[35] I. A. Kadoma, C. Ylitalo, J. W. v. Egmond, Rheol. Acta 36 (1997) 1-12.

[36] S. Puvvada, D. Blankschtein, J. Chem. Phys. 92 (1990) 3710.

[37] A. Bernheim-Groswasser, E. Wachtel, Y. Talmon, Langmuir, 16 (2000) 4131-4140.

[38] A. Zilman, S. A. Safran, T. Stottmann, R. Strey, Langmuir 20 (2004) 2199-2207.

[39] T. Tlusty, S. A. Safran, Science 290 (2000) 1328.

Chapter 5: Conclusions

Poly(oxyethylene) cholesteryl ethers are unique among the POE nonionic surfactants in being able to form highly viscous aqueous micellar solutions. Even with EO chain of 30, it is possible to form solution with $\sim10^3$ Pa·s zero-shear viscosity by adding appropriate cosurfactant, namely $C_{12}EO_3$. To date, such highly viscous solutions have not been reported in the case of Poly (oxyethylene) alkyl ether surfactants, the most common type of POE surfactant.

In Chapter 3 we have seen that changing the headgroup size of poly(oxyethylene) cholesteryl ether from 30 to 15 has the effect of less cosurfactant requirement for micellar growth. The explanation invoked is that the interface of larger headgroup surfactant micelle is more curved and therefore more cosurfactant is needed for sufficient curvature reduction to allow wormlike micelle formation. It is scientifically satisfying to find that the concept of interfacial curvature reduction is useful even in the case of such long poly(oxyethylene) chain surfactants. The agreement of rheological data with Maxwell model, as predicted by Cates' theory, implies that now the systematic headgroup size variation of surfactant molecules is another tunable parameter, besides the usual factors such as salt content, surfactant concentration, temperature etc., for deeper experimental study of the structure and dynamics of wormlike micellar solution. Since the cosurfactant headgroup should be small enough so that it is hydrophobic, we do not have a large range of cosurfactant headgroup sizes to vary. But now from our investigations, we see that the headgroup size can be quite extensively varied. We have also seen that the effectiveness of cosurfactants such as $C_{12}EO_3$ or monolaurin in promoting micellar growth cannot be placed in any invariable order but rather is dependent upon the particular system to

which these are added. Thus, there is no hard-and-fast rule for cosurfactant selection for micellar growth.

In Chapter 4 we look at the temperature dependence of poly(oxyethylene) cholesteryl ether surfactant micellar solution viscosity for different cosurfactants. Since POE chains are dehydrated at high temperature, and therefore micellar interfacial curvature is reduced, it is expected that the poly(oxyethylene) cholesteryl ether micelles would grow with temperature rise and the solution viscosity increase, as opposed to the well-studied ionic surfactant wormlike micelles, whose solution viscosity decrease with temperature rise due to the reduction of the micellar length. Indeed, we find that the curvature reduction can induce micellar branching following growth, resulting in a maximum in viscosity-temperature plot. Again, we see that the exact behavior depends on the particular cosurfactant used. However, in general we find that the temperature sensitivity of micellar solution viscosity decreases as we go from POE chain length 15 to 30. In the case of $C_{12}EO_3$ containing solutions, detailed dynamic rheological study strongly suggests that the temperature induced curvature reduction of the interface of POE surfactants is responsible for the observed behavior.

In summary, we can say that with poly(oxyethylene) cholesteryl ether surfactants we can form very viscous wormlike micellar solution in long POE chain surfactant solution upon greater amount of cosurfactant compared to shorter POE chain surfactant and the temperature-sensitivity of the rheology of such solutions can be significantly reduced when the POE chain is very long. We expect that this concept can be utilized to develop completely temperature-insensitive wormlike micellar solution in the future.